IEEE Access
Multidisciplinary | Rapid Review | Open Access Journal

Received September 28, 2019, accepted October 12, 2019, date of publication October 21, 2019, date of current version October 31, 2019.

Digital Object Identifier 10.1109/ACCESS.2019.2948403

Performance Analysis of Gini Correlator for Detecting Known Signals in Impulsive Noise

CHANGRUN CHEN[1], WEICHAO XU[1], (Member, IEEE), JISHENG DAI[2], (Member, IEEE), YANZHOU ZHOU[1], AND YUN ZHANG[1]

[1]Department of Automatic Control, School of Automation, Guangdong University of Technology, Guangzhou 510006, China
[2]School of Electrical and Information Engineering, Jiangsu University, Zhenjiang 212013, China

Corresponding author: Weichao Xu (wcxu@gdut.edu.cn)

This work was supported in part by the National Natural Science Foundation of China under Project 61771148, Project 61571211, Project U1501251, and Project 61875041.

ABSTRACT Detection of known signals embedded in additive noise is a fundamental problem in signal processing. For normally distributed noise, it is well known that the popular matched filter detector (MFD) is optimal. However, for impulsive noise whose distribution has a heavier tail, the performance of MFD will deteriorate severely. To deal with such problem, in this paper, we propose a novel detector, termed as Gini correlator (GC), and derive the analytic forms of its expectation and variance, under a specified contaminated Gaussian model (CGM) emulating a frequently encountered scenario in practice. In order to further understand its properties, we compare the proposed GC with five state-of-the-art detectors permeating in the literature, in terms of Pitman asymptotic relative efficiency (ARE), as well as time-delay estimation. Monte Carlo simulations not only validate our theoretical discoveries, but also demonstrate the advantages of GC in the aspects of 1) accurate control of false alarm probability without prior knowledge of noise distribution, 2) comparable performance with MFD for Gaussian noise, 3) better performances over the classical detectors in the aspects of greater ARE and smaller bias and standard deviation for time-delay estimation. The theoretical and empirical findings in this work enable GC to be a useful alternative to the existing detectors whether or not impulsivity exists in noise.

INDEX TERMS Gini correlator (GC), Kendall's tau (KT), locally optimal detector (LOD), Pitman asymptotic relative efficiency (ARE), sign correlator (SC), Spearman's rho (SR).

I. INTRODUCTION

Detecting whether or not a known signal is embedded in noise is one of the most basic and important problems in the area of signal processing [1]–[6]. In radar, for example, the detection procedure is as follows. Firstly, a prescribed electromagnetic pulse, of known mathematical form, is transmitted from the antenna. Then, after obtaining the observed waveform at the receiver end, two situations might arise: 1) if the target is present, the observed waveform will contain an attenuated version of the transmitted pulse along with the noise resulting from ambient radiation and the receiver electronics; 2) if the target is not present, then only the noise term remains in the observed signal [7]. Given the received signal, the detection problem is further cast into a binary hypothesis test, i.e., target present vs. target absent, based on some statistic from the observed data. Finally, an appropriate threshold is derived according to some optimal criterion, such as the well known Neyman-Pearson theorem [7].

In the above mentioned scenario, the noise is usually assumed to be independently and identically distributed (i.i.d.) Gaussian (white Gaussian nose) for the reasons of central limit theorem [8] and mathematical tractability [9]. It is well known that the matched filter detector (MFD) is optimal, in the sense of maximizing the output signal to noise ratio (SNR), when the additive noise is white Gaussian [7]. However, the model of white Gaussian noise is too restrictive for many real world scenarios. Theoretical and empirical evidences show that impulsive noise appears in a variety of applications such as wireless communications, radar, sonar and image processing [10]. For those impulsive noises whose probability density function (pdf) possesses a heavier tail than that of Gaussian, the performance of MFD will deteriorate severely.

The associate editor coordinating the review of this manuscript and approving it for publication was Khaled Rabie.

To avoid the sensitivity of the MFD to impulsive noise, many efforts have been made by practitioners in the area of signal processing [11]–[17]. The basic idea behinds the existing methods is to suppress the influence of large-valued data contained in observed signal. By imposing various nonlinearities on the observed signal, researchers have devised a lot of robust detectors, including the locally optimal detector (LOD) [7], threshold-system-based detector (TD) [18], gaussianization and generalized matching (GGM) [19], limiter-correlator (LC) [20], sign correlator (SC) [21], Spearman's rho (SR) [22], and Kendall's tau (KT) [22] among others.

There are many advantages and disadvantages to the methods just mentioned. The LOD is nearly optimal when the SNR is low, but its implementation demands knowing exactly the noise pdf, which is usually impossible in practice. The TD and GGM are asymptotically optimal under the assumptions of the noise with a symmetric and unimodal pdf [18]. However, the asymptotic optimality of TD and GGM might be destroyed if the assumptions do not hold true. The LC detector, while being the locally most powerful detector under some mild conditions, requires the full knowledge of noise pdf, which is seldom realistic in real-world problems [23]. The SC detector, on the other hand, is the most robust detector when the majority of noise follows the Laplace distribution [24]. Nevertheless, using only the information of algebraic signs of the observed signal, the SC detector might not perform well when the noise distribution is nearly Gaussian with only a tiny fraction of impulsive component. The two rank-based detectors, namely SR and KT, are well known to be distribution-free in the null case (when the target is absent) [22], which makes it convenient to control the false alarm probability. However, dropping the cardinal information contained in the known transmitted signal, SR and KT will unavoidably lose detection power, especially when the tail of noise distribution is not very heavy. Moreover, unlike SR and KT, the null distributions of LOD, TD, LC, SC, and MFD are all dependent on the parameters of noise pdf. This makes it hard to accurately control the false alarm probability without knowledge of noise pdf.

To overcome the drawbacks of the above mentioned methods, in this paper we propose a robust detector based on the ranks of the observed signal and the variates of the known transmitted signal. Since its mathematical expression is the numerator of the Gini correlation [25]–[28], we name our proposed detector as Gini correlator (GC) throughout this work. As to be illustrated later on, from both theoretical and empirical viewpoints based on a contaminated Gaussian model (CGM) emulating impulsive noise, GC possesses the following advantages: 1) it is distribution free in the null case, that is, the mean and variance of GC depend only on the signal length, 2) it does not require the noise pdf to be symmetric and unimodal, 3) in the normal case where MFD is optimal, the Pitman asymptotic relative efficiency (ARE) [29] of GC to MFD is $3/\pi$ when the signal is weak, and 4) it consistently outperforms SC, SR and KT under the contaminated Gaussian model (CGM) described in (3), and performs only slightly worse than LOD, which is theoretically optimal in low SNR cases.

Our contribution in this work is fourfold. Firstly, we prove that, in the null case (when the target is absent), the expectation and variance of GC is independent of the distribution of noise. This property, along with the central limit theorem [8], allows us to control the false alarm rate accurately without knowing the functional form of noise pdf. Secondly, we established the closed forms of the expectation and variance of GC under the CGM (3). These theoretical results, together with the central limit theorem again, allow us to work on performance analysis, such as computation of efficacy and efficiency, by approximating the distribution of GC with Gaussian distribution when the sample size is relatively large. Thirdly, we derive the Pitman ARE [29] of GC to MFD when the noise is assumed to be i.i.d. Gaussian and the signal is weak. This result, to some degree, justifies the comparable performances of GC and MFD, in terms of detection probability, when the noise is white Gaussian, a scenario in favor of MFD. Fourthly, we establish the analytical expressions of the mean and variance of SC, under the specific CGM (3). These theoretical results on SC are not only of interest on their own, but also indispensable for performance evaluation.

The remainder of this paper is organized as follows. Section II describes the problem formulation including the additive model and the CGM modeling the impulsive noise. Section III presents some basic definitions and properties concerning GC, MFD, LOD, SR and KT, laying the foundation for further analyses. In section IV, we establish our major theoretical results, i.e., the analytic expressions of the mean and variance of GC under the CGM model. Moreover, some corollaries helpful for further understanding of GC are also established. Section V establishes the theoretical results of the mean and variance of SC under the CGM model. The Pitman ARE of SC with respect to MFD in the normal case is also derived in the same section. In section VI, we verify our theoretical findings and compare GC with LO, MFD, SC, SR and KT via a series of extensive Monte Carlo simulations. Finally, in section VII, we summarize our main findings and our conclusion on the proposed Gini Correlator.

For convenience in the following discussion, throughout we employ the symbols $\mathbb{E}(\cdot)$, $\mathbb{V}(\cdot)$ and $\mathbb{C}(\cdot,\cdot)$ to denote the mean, variance and covariance of (between) random variables, respectively. Moreover, $\Phi(t)$ and $\phi(t)$ represent the cumulative distribution function (cdf) and pdf of the univariate standard normal distribution, respectively; whereas $\Psi(u, v, \rho)$ represents the cdf of the bivariate standard normal distribution with correlation ρ. The symbol $\Pr(\cdot)$ denotes the probability that the event inside the brackets occurs. The sign "$\triangleq$" stands for "is defined as", whereas "$\sim$" reads "obey to". All other notation is to be defined in the context where it first enters.

II. PROBLEM FORMULATION

A. DETECTION MODEL

The detection problem is often formulated as [7]

$$X[i] = \lambda y[i] + Z[i] \tag{1}$$

where $y[i]$ is deterministic corresponding the transmitted electromagnetic pulse, λ is the strength coefficient representing the presence ($\lambda \neq 0$) or absence ($\lambda = 0$) of the target, $Z[i]$ is the noise term emulating the interference due to ambient radiation and/or the receiver electronics, and $X[i]$ represents the received waveform. Note that, for mathematical tractability, the noise $Z[i]$ is often assumed to be an independent and identically distributed (i.i.d.) sample drawn from some continuous distribution (such as normal distribution) in the literature [7]. The signal terms $X[i]$, $y[i]$ and $Z[i]$ in (1) are abbreviated as X_i, y_i, and Z_i, respectively, for compactness. Given the additive model of (1), the detection problem can then be cast into the following binary hypothesis test:

$$\begin{cases} H_1 : \lambda \neq 0 \text{ (target present)} \\ H_0 : \lambda = 0 \text{ (target absent)} \end{cases} \tag{2}$$

If the functional pdf of Z in (1) is known, an optimal detector, called log-likehood ratio (LLR) detector, can be established, as [30]

$$T(x) = \log\left[\frac{f(x|H_1)}{f(x|H_0)}\right]$$

where $f(x|H_r)$ is the pdf of the observed signal X under Hypothesis H_r, $r = 0, 1$. An appropriate threshold η, say, is derived base on some optimal criterion, such as the famous Neyman-Pearson criterion [7]. The corresponding detector decides on H_0 if $T(x) \leq \eta$ and H_1 otherwise. Since the LLR above requires full knowledge of noise pdf in advance, it is seldom practical in scenarios where noise pdf is unknown.

B. CONTAMINATED GAUSSIAN MODEL

To simulate the impulsive noise encountered in real world problems, various models have been proposed in the literature. Among them, the symmetric α-stable (SαS) distribution noise model and the Middleton Class A noise model have been widely used due to excellent agreements with measurement data [31]–[33]. However, lacking the closed-form pdfs, these two kinds of impulsive noise models are mathematically rather intractable. For ease of mathematical treatment, many mixture models that emulate impulsive noise are proposed [34]–[37], among which, the contaminated Gaussian model (CGM) is perhaps the most popular. Therefore, in this work, we employ the following contaminated Gaussian model [38]

$$f_Z(z) = \frac{1-\varepsilon}{\sqrt{2\pi}\sigma_1}\exp\left[-\frac{(z-\mu_1)^2}{2\sigma_1^2}\right] + \frac{\varepsilon}{\sqrt{2\pi}\sigma_2}\exp\left[-\frac{(z-\mu_2)^2}{2\sigma_2^2}\right] \tag{3}$$

where $f_Z(z)$ stands for the pdf of noise Z_i, $0 < \varepsilon \ll 1$, $\sigma_2 \to \infty$. Note that the pdf above contains two Gaussian components: the first one represents the distribution of the majority of the data, with limited variance; whereas the second one, with a tiny fraction of ε, represents the distribution of a minority of outliers with very large variance.

III. PRELIMINARIES

This section presents 1) the definitions of ranks and the proposed GC, 2) definitions of other five detectors to be compared in this work, namely, LOD, MFD, SC, SR and KT, and 3) some auxiliary lemmas for ease of following expositions.

A. DEFINITIONS OF GC AND OTHER DETECTORS

1) GINI CORRELATOR

Let $\{X_i\}_{i=1}^n$ denote the observed signal of length n in (1). Rearranging $\{X_i\}_{i=1}^n$ in ascending order yields a new sequence of $X_{(1)} < \ldots < X_{(n)}$, which is termed the order statistic of X [39]–[43]. Suppose that X_j is at the kth position in the sorted sequence $\{X_{(i)}\}_{i=1}^n$. The position index $k \in [1\ n]$ is termed the rank of X_j and is denoted by P_j. Similarly we can also obtain the rank of y_i denoted by q_i for $i = 1, \ldots, n$. The proposed Gini correlator is defined as

$$T_{\mathrm{GC}} \triangleq \sum_{i=1}^{n}(2P_i - 1 - n)y_i, \tag{4}$$

which is the numerator of the Gini correlation [25]–[28].

2) MATCHED FILTER BASED DETECTOR

The matched filter based detector is simply the following inner product form [11]

$$T_{\mathrm{MF}} \triangleq \sum_{i=1}^{n} X_i y_i. \tag{5}$$

3) LOCALLY OPTIMAL DETECTOR

The locally optimal detector (LOD) is defined as [11]

$$T_{\mathrm{LO}} \triangleq \sum_{i=1}^{n} L(X_i)y_i \tag{6}$$

where

$$L = -\frac{f'(X_i)}{f(X_i)} \tag{7}$$

with $f(\cdot)$ being the pdf of Z_i. Note that when X_i is strictly normal, or, equivalently, Z_i is strictly normal, i.e., when $\varepsilon = 0$ in (3), T_{LO} reduces to T_{MF} except for a possible constant multiplicative factor.

4) SIGN CORRELATOR

The sign correlator is defined as [24]

$$T_{\mathrm{SC}} \triangleq \sum_{i=1}^{n} \mathrm{sign}(X_i)y_i \tag{8}$$

where sign$(\cdot)$ represents the algebra sign of the argument.

5) SPEARMAN'S RHO

The first rank-based detector, known as Spearman's rho, is defined as [44]

$$T_{\mathrm{SR}} \triangleq 1 - \frac{6}{n(n^2-1)} \sum_{i=1}^{n} (P_i^2 - q_i^2). \tag{9}$$

6) KENDALL'S TAU

The other rank-based detector, known as Kendall's tau, is defined as [44]

$$T_{\mathrm{KT}} \triangleq \frac{1}{n(n-1)} \sum_{i \neq j=1}^{n} \sum^{n} \mathrm{sign}(X_i - X_j)(y_i - y_j). \tag{10}$$

B. AUXILIARY RESULTS CONCERNING GC

Lemma 1: The Gini correlator defined in (4) can be expressed in the following form

$$T_{\mathrm{GC}} = \sum_{i \neq j=1}^{n} \sum^{n} H(X_i - X_j)(y_i - y_j) \tag{11}$$

where $H(t) = 1$ for $t > 0$ and $H(t) = 0$ for $t \leq 0$.

Proof: See Appendix A. □

Remark 1: As shown in Appendix A, (4) and (11) are mathematically equivalent. However, they are of different usefulness according to different purposes. Formula (4), with a linearithmic time complexity of order $n \log(n)$, is more convenient in the aspect of computation; whereas (11), although with a quadratic time complexity, is more convenient in the aspect of analysis.

Lemma 2: Assume that $\{Z_i\}_{i=1}^n$ are i.i.d. random variables obeying some continuous distribution. Let

$$H_{ij} \triangleq H(X_i - X_j) \tag{12}$$

$$\Delta_{ij} \triangleq y_i - y_j \tag{13}$$

Then,

$$\mathbb{E}(T_{\mathrm{GC}}) = \sum_{i \neq j=1}^{n} \sum^{n} \mathbb{E}(H_{ij}) \Delta_{ij} \tag{14}$$

$$\mathbb{V}(T_{\mathrm{GC}}) = 2 \sum_{i \neq j=1}^{n} \sum^{n} \mathbb{V}(H_{ij}) \Delta_{ij}^2 + 4 \sum_{i \neq j \neq k=1}^{n} \sum^{n} \sum^{n} \mathbb{C}(H_{ij}, H_{ik}) \Delta_{ij} \Delta_{ik}. \tag{15}$$

Proof: See Appendix B. □

Lemma 3: Assume that $\{Z_i\}_{i=1}^n$ are i.i.d. random variables obeying some continuous distribution. Then, for $\lambda = 0$ in (1),

$$\mathbb{E}(T_{\mathrm{GC}}) = 0 \tag{16}$$

$$\mathbb{V}(T_{\mathrm{GC}}) = \frac{1}{2} \sum_{i \neq j=1}^{n} \sum^{n} \Delta_{ij}^2 + \frac{1}{3} \sum_{i \neq j \neq k=1}^{n} \sum^{n} \sum^{n} \Delta_{ij} \Delta_{ik} \tag{17}$$

$$= \frac{n+1}{6} \sum_{i \neq j=1}^{n} \sum^{n} (y_i - y_j)^2 \tag{18}$$

$$= \frac{n+1}{3} \left[n \sum_{i=1}^{n} y_i^2 - \left(\sum_{i=1}^{n} y_i \right)^2 \right]. \tag{19}$$

Proof: See Appendix C. □

Remark 2: The results with respect to the null case are independent of the specific distribution form of $\{Z_i\}_{i=1}^n$. This desirable property of GC allows us to accurately control the false alarm probability by assuming that, as n large,

$$T_{\mathrm{GC}} \sim \mathcal{N}\left(0, \frac{n+1}{6} \sum_{i \neq j=1}^{n} \sum^{n} \Delta_{ij}^2\right) \tag{20}$$

due to the well known central limit theorem [8].

Lemma 4: Let $\xi_\ell \sim \mathcal{N}(\nu_\ell, \varsigma_\ell^2)$, $\ell = 1, 2, 3$ be three mutually independent normal random variables. Write $\Delta\nu_{12} \triangleq \nu_1 - \nu_2$, $\Delta\nu_{13} \triangleq \nu_1 - \nu_3$, $\varsigma_{12}^2 \triangleq \varsigma_1^2 + \varsigma_2^2$, $\varsigma_{13}^2 \triangleq \varsigma_1^2 + \varsigma_3^2$, $\Delta\xi_{12} \triangleq \xi_1 - \xi_2$, and $\Delta\xi_{13} \triangleq \xi_1 - \xi_3$. Then

$$\mathbb{E}[H(\Delta\xi_{12})] = \Phi\left(\frac{\Delta\nu_{12}}{\varsigma_{12}}\right) \tag{21}$$

$$\mathbb{E}[H(\Delta\xi_{12})H(\Delta\xi_{13})] = \Psi\left(\frac{\Delta\nu_{12}}{\varsigma_{12}}, \frac{\Delta\nu_{13}}{\varsigma_{13}}, \frac{\varsigma_1^2}{\varsigma_{12}\varsigma_{13}}\right). \tag{22}$$

Proof: See Appendix D. □

C. MEAN AND VARIANCE OF MFD IN GENERAL CASE

Lemma 5: Assume that $\{Z_i\}_{i=1}^n$ are i.i.d. random variables with $\mathbb{E}(Z_i) = \mu_Z$ and $\mathbb{V}(Z_i) = \sigma_Z^2$. Then, under the model (1), the mean and variance of T_{MF} defined in (5) are

$$\mathbb{E}(T_{\mathrm{MF}}) = \lambda \sum_{i=1}^{n} y_i^2 + \mu_Z \sum_{i=1}^{n} y_i \tag{23}$$

$$\mathbb{V}(T_{\mathrm{MF}}) = \sigma_Z^2 \sum_{i=1}^{n} y_i^2. \tag{24}$$

Proof: See Appendix E. □

Remark 3: The mean and variance of T_{MF} both depend on the parameters of Z, even when $\lambda = 0$. This means that we have to estimate μ_Z and σ_Z in practice before determining the threshold of the detector based on T_{MF}. In other words, the false alarm probability is controlled based on the assumption that, as n large,

$$T_{\mathrm{MF}} \sim \mathcal{N}\left(\hat{\mu}_Z, \hat{\sigma}_Z^2 \sum_{i=1}^{n} y_i^2\right) \tag{25}$$

where $\hat{\mu}_Z$ and $\hat{\sigma}_Z^2$ are estimates based on the observed data.

D. MEAN AND VARIANCE OF SR AND KT IN NULL CASE

Lemma 6: Assume that $\{Z_i\}_{i=1}^n$ are i.i.d. random variables obeying some continuous distribution. Then, for $\lambda = 0$ in (1),

$$\mathbb{E}(T_{\mathrm{SR}}) = 0 \tag{26}$$

$$\mathbb{V}(T_{\mathrm{SR}}) = \frac{1}{n-1} \tag{27}$$

$$\mathbb{E}(T_{\mathrm{KT}}) = 0 \tag{28}$$

$$\mathbb{V}(T_{\mathrm{KT}}) = \frac{2}{9}\frac{2n+5}{n(n-1)}. \tag{29}$$

Proof: See [22]. □

IV. PROPERTIES OF GINI CORRELATOR UNDER CONTAMINATED GAUSSIAN MODEL

In this section we establish our major results about the statistical properties of the Gini correlator under the contaminated Gaussian model. Below we focus on the expressions of the mean and variance of GC under the CGM, since, according to the central limit theorem, GC asymptotically can be well approximated by a normal distribution that requires only the first two moments. As shown in Theorem 1 below, both the expectation and variance of GC exhibit robustness against the impulsive noise modeled by (3) in Section I.

A. EXPECTATION AND VARIANCE OF GC UNDER CGM

Theorem 1: Let $\{(X_i, y_i, Z_i)\}_{i=1}^n$ satisfy the data model presented in (1), where $\{Z_i\}_{i=1}^n$ are i.i.d. random variables following the distribution of (3). Let H_{ij} and Δ_{ij} be the same as in (12) and (13), respectively. Write

$$\Phi_{ij} \triangleq \Phi\left(\frac{\lambda\Delta_{ij}}{\sqrt{2}\sigma_1}\right) \tag{30}$$

$$\Psi_{ijk} \triangleq \Psi\left(\frac{\lambda\Delta_{ij}}{\sqrt{2}\sigma_1}, \frac{\lambda\Delta_{ik}}{\sqrt{2}\sigma_1}, \frac{1}{2}\right). \tag{31}$$

Denote by $\phi_\ell(\cdot)$ the pdf of $\mathcal{N}(\lambda y_\ell + \mu_1, \sigma_1^2)$ and $\psi_\ell(\cdot)$ the pdf of $\mathcal{N}(\lambda y_\ell + \mu_2, \sigma_2^2)$, where $\ell \in \{i, j, k\}$. Let $\Delta\mu \triangleq \mu_1 - \mu_2$. Then, as $\sigma_2 \to \infty$, the expectation and variance of T_{GC} defined in (4) are, respectively,

$$\mathbb{E}(T_{\mathrm{GC}}) = (1-\varepsilon)^2 \sum_{i\neq j=1}^{n}\sum^{n} \Phi_{ij}\Delta_{ij} \tag{32}$$

$$\begin{aligned}\mathbb{V}(T_{\mathrm{GC}}) &= 2(1-\varepsilon)^4 \sum_{i\neq j=1}^{n}\sum^{n} \Phi_{ij}(1-\Phi_{ij})\Delta_{ij}^2 \\ &\quad + \frac{1}{2}[1-(1-\varepsilon)^4]\sum_{i\neq j=1}^{n}\sum^{n}\Delta_{ij}^2 \\ &\quad + 4(1-\varepsilon)^3 \sum_{i\neq j\neq k=1}^{n}\sum^{n}\sum^{n} \left(\Psi_{ijk} - \Phi_{ij}\Phi_{ik}\right)\Delta_{ij}\Delta_{ik} \\ &\quad + 4\varepsilon(1-\varepsilon)^3 \sum_{i\neq j\neq k=1}^{n}\sum^{n}\sum^{n} \left(\Phi_{ij} - \frac{1}{2}\right) \\ &\quad \times \left(\Phi_{ik} - \frac{1}{2}\right)\Delta_{ij}\Delta_{ik} \\ &\quad + \frac{1}{3}[1-(1-\varepsilon)^3]\sum_{i\neq j\neq k=1}^{n}\sum^{n}\sum^{n}\Delta_{ij}\Delta_{ik}.\end{aligned} \tag{33}$$

Proof: See Appendix F. □

Corollary 1: The expectation $\mathbb{E}(T_{\mathrm{GC}})$ in (32) is odd symmetric with respect to λ; whereas the variance $\mathbb{V}(T_{\mathrm{GC}})$ in (33) is even symmetric with respect to λ.

Proof: See Appendix G. □

B. EXPECTATION AND VARIANCE OF GC IN PARTICULAR CASES

Given the results established in Theorem 1, some corollaries follow readily as shown below.

Corollary 2: In the null case, i.e., when $\lambda = 0$, the expressions of $\mathbb{E}(T_{\mathrm{GC}})$ and $\mathbb{V}(T_{\mathrm{GC}})$ in (32) and (33) degenerate to those of (16) and (17), respectively.

Proof: Substituting $\lambda = 0$ in (32) and (33) along with the results

$$\Phi(0) = \frac{1}{2} \tag{34}$$

$$\Psi\left(0, 0, \frac{1}{2}\right) = \frac{1}{3} \tag{35}$$

gives

$$\mathbb{E}(T_{\mathrm{GC}})|_{\lambda=0} = (1-\varepsilon)^2 \sum_{i\neq j=1}^{n}\sum^{n}\frac{1}{2}\Delta_{ij} = 0 \tag{36}$$

$$\mathbb{V}(T_{\mathrm{GC}})|_{\lambda=0} = \frac{1}{2}\sum_{i\neq j=1}^{n}\sum^{n}\Delta_{ij}^2 + \frac{1}{2}\sum_{i\neq j\neq k=1}^{n}\sum^{n}\sum^{n}\Delta_{ij}\Delta_{ik} \tag{37}$$

which are the results corresponding (16) and (17) in Lemma 3 for the null case. □

Corollary 3: For $\{Z_i\}_{i=1}^n$ being i.i.d. normal random variables, that is, $\varepsilon \to 0$ in Theorem 1, $\mathbb{E}(T_{\mathrm{GC}})$ and $\mathbb{V}(T_{\mathrm{GC}})$ reduce respectively to

$$\mathbb{E}(T_{\mathrm{GC}}) = \sum_{i\neq j=1}^{n}\sum^{n}\Phi_{ij}\Delta_{ij} \tag{38}$$

and

$$\begin{aligned}\mathbb{V}(T_{\mathrm{GC}}) &= 2\sum_{i\neq j=1}^{n}\sum^{n}\Phi_{ij}(1-\Phi_{ij})\Delta_{ij}^2 \\ &\quad + 4\sum_{i\neq j\neq k=1}^{n}\sum^{n}\sum^{n}(\Psi_{ijk} - \Phi_{ij}\Phi_{ik})\Delta_{ij}\Delta_{ik}.\end{aligned} \tag{39}$$

Proof: The results follows directly by letting $\varepsilon = 0$ in (32) and (33), respectively. □

Remark 4: It is not difficult to verify that, upon substitution of $\lambda = 0$, (38) and (39) reduce also to (16) and (17) in Lemma 3, respectively.

Corollary 4: Assume that $\{Z_i\}_{i=1}^n$ are i.i.d. normal random variables, that is, $\varepsilon \to 0$ in Theorem 1. Then, as $\lambda/\sigma_1 \to \pm\infty$, $\mathbb{E}(T_{\mathrm{GC}})$ and $\mathbb{V}(T_{\mathrm{GC}})$ tend respectively to

$$\lim_{\frac{\lambda}{\sigma_1}\to\pm\infty} \mathbb{E}(T_{\mathrm{GC}}) = \pm\frac{1}{2}\sum_{i\neq j=1}^{n}\sum^{n}|\Delta_{ij}| \tag{40}$$

and

$$\lim_{\frac{\lambda}{\sigma_1}\to\pm\infty} \mathbb{V}(T_{\mathrm{GC}}) = 0. \tag{41}$$

Proof: It follows that

$$\begin{aligned}\lim_{\frac{\lambda}{\sigma_1}\to+\infty} \Phi\left(\frac{\lambda\Delta_{ij}}{\sqrt{2}\sigma_1}\right) &= \begin{cases}1 & \text{for } \Delta_{ij} > 0 \\ \frac{1}{2} & \text{for } \Delta_{ij} = 0 \\ 0 & \text{for } \Delta_{ij} < 0\end{cases} \\ &= \frac{1}{2} + \frac{1}{2}\mathrm{sign}(\Delta_{ij})\end{aligned} \tag{42}$$

and hence

$$\lim_{\frac{\lambda}{\sigma_1}\to-\infty}\Phi\left(\frac{\lambda\Delta_{ij}}{\sqrt{2}\sigma_1}\right)=\frac{1}{2}-\frac{1}{2}\text{sign}(\Delta_{ij}) \tag{43}$$

which mean that

$$\lim_{\frac{\lambda}{\sigma_1}\to\pm\infty}\mathbb{E}(T_{\text{GC}})=\pm\frac{1}{2}\sum_{i\neq j=1}^{n}\sum^{n}\text{sign}(\Delta_{ij})\Delta_{ij}+\underbrace{\frac{1}{2}\sum_{i\neq j=1}^{n}\sum^{n}\Delta_{ij}}_{=0}$$

$$=\pm\frac{1}{2}\sum_{i\neq j=1}^{n}\sum^{n}|\Delta_{ij}|$$

being consistent with (40).

By the reduction formula in [45],

$$\Psi_{ijk}-\Phi_{ij}\Phi_{ik}$$

$$=\frac{1}{2\pi}\int_0^1\frac{dr}{\sqrt{1-r^2}}\exp\left\{-\frac{\lambda^2}{2\sigma_1^2}\frac{\Delta_{ij}^2-2r\Delta_{ij}\Delta_{ik}+\Delta_{ik}^2}{2(1-r^2)}\right\}$$

$$\to 0 \text{ as } \frac{\lambda}{\sigma_1}\to\pm\infty. \tag{44}$$

Substituting (42)–(44) into (39) leads readily to the result of (41). □

Remark 5: The results just established in Corollary 4 suggest that it is reasonable to define the signal to noise ratio as

$$\text{SNR}\triangleq\frac{\lambda}{\sigma_1}. \tag{45}$$

The larger the magnitude of SNR, the larger the magnitude of $\mathbb{E}(T_{\text{GC}})$ *and the smaller the value of* $\mathbb{V}(T_{\text{GC}})$*. This means that with increase of SNR, the detection probability increases accordingly.*

Corollary 5: In the extreme case of $\varepsilon\to 1$*, the expressions of* $\mathbb{E}(T_{\text{GC}})$ *and* $\mathbb{V}(T_{\text{GC}})$ *in (32) and (33) degenerate also to those of (16) and (17), respectively.*

Proof: The results follows directly by letting $\varepsilon\to 1$ in (32) and (33), respectively. □

C. ASYMPTOTIC RELATIVE EFFICIENCIES IN NORMAL CASE

Here we employ the asymptotic relative efficiency (ARE), in Pitman's sense, as the figure of merit for the purpose of comparison. Under mild regularity conditions, the ARE of Detector A to Detector B is given by the ratio of their efficacies [29]

$$\text{ARE}_{\text{A,B}}\triangleq\frac{\mathcal{E}_{\text{A}}}{\mathcal{E}_{\text{B}}} \tag{46}$$

with efficacy terms $\mathcal{E}$ being defined as

$$\mathcal{E}_{\zeta}=\left[\frac{\mathbb{E}'(T_{\zeta})}{\sqrt{V(T_{\zeta})}}\right]^2 \tag{47}$$

where the subscript $\zeta\in\{\text{LO, GC, MF, SR, KT, SC}\}$, and the derivatives are with respect to λ.

As remarked in Section I, T_{MF} is optimal when $\{Z_i\}_{i=1}^n$ are i.i.d. Gaussian. Therefore, it is of interest to investigate the efficiency loss of T_{GC} in this case which is in favor of T_{MF}. As shown in Corollary 6 below, T_{GC} is asymptotically about $3/\pi(\simeq 95\%)$ as efficient as T_{MF} when the known signal y has no DC component and the noise is white Gaussian.

Corollary 6: Let $\{(X_i,y_i,Z_i)\}_{i=1}^n$ *satisfy the data model presented in (1), where* $\{Z_i\}_{i=1}^n$ *are i.i.d. random variables following the normal distribution of* $\mathcal{N}(\mu_1,\sigma_1^2)$*. Then the Pitman ARE of* T_{GC} *to* T_{MF} *for weak signals* ($\lambda\to 0$) *is*

$$\text{ARE}_{\text{GC,MF}}=\frac{3}{\pi}\frac{n}{n+1}\frac{\sum_{i=1}^n y_i^2-\frac{1}{n}\left(\sum_{i=1}^n y_i\right)^2}{\sum_{i=1}^n y_i^2} \tag{48}$$

Proof: By Lemma 5, Corrolary 3 and Lemma 3, it follows that

$$\lim_{\lambda\to 0}\mathbb{E}'(T_{\text{MF}})=\sum_{i=1}^n y_i^2 \tag{49}$$

$$\lim_{\lambda\to 0}\mathbb{V}(T_{\text{MF}})=\sigma_1^2\sum_{i=1}^n y_i^2 \tag{50}$$

$$\lim_{\lambda\to 0}\mathbb{E}'(T_{\text{GC}})=\frac{1}{2\sqrt{\pi}\sigma_1}\sum_{i\neq j=1}^{n}\sum^{n}\Delta_{ij}^2 \tag{51}$$

$$\lim_{\lambda\to 0}\mathbb{V}(T_{\text{GC}})=\frac{n+1}{3}\left[n\sum_{i=1}^n y_i^2-\left(\sum_{i=1}^n y_i\right)^2\right]. \tag{52}$$

The result of (48) follows readily by substituting (49)–(52) into (46). □

Remark 6: It is obvious that the ARE reaches maximum value when $\sum y_i=0$ *in (48), being*

$$\text{ARE}_{\text{GC,MF}}=\frac{n}{n+1}\frac{3}{\pi}\to\frac{3}{\pi}\ \textit{as}\ n\to\infty \tag{53}$$

which suggests that, to enhance the performance of T_{GC}*, one should remove the arithmetic average from the designed signal* $\{y_i\}_{i=1}^n$*. It is noteworthy that* ARE $=0$ *when* $y_i=$ constant*. In other words, it is unsuitable to apply* T_{GC} *to detecting the presence of constant signals in practice.*

V. MEAN AND VARIANCE OF SIGN CORRELATOR UNDER CONTAMINATED GAUSSIAN MODEL

This section establishes the analytical results of the mean and variance of SC under the CGM in (3). These results, as remarked before, are not only of interest on their own, but also helpful for plotting the ARE curves. The Pitman ARE of SC to MFD in the normal case is also established for weak signals ($\lambda\to 0$).

A. MEAN AND VARIANCE OF SC

Theorem 2: Let $\{(X_i,y_i,Z_i)\}_{i=1}^n$ *satisfy the data model presented in (1), where* $\{Z_i\}_{i=1}^n$ *are i.i.d. random variables following the distribution of (3). Let* T_{SC} *be defined as in (8). Then*

$$\mathbb{E}(T_{\text{SC}})=(1-\varepsilon)\sum_{i=1}^n\left[2\Phi\left(\frac{\lambda y_i+\mu_1}{\sigma_1}\right)-1\right]y_i \tag{54}$$

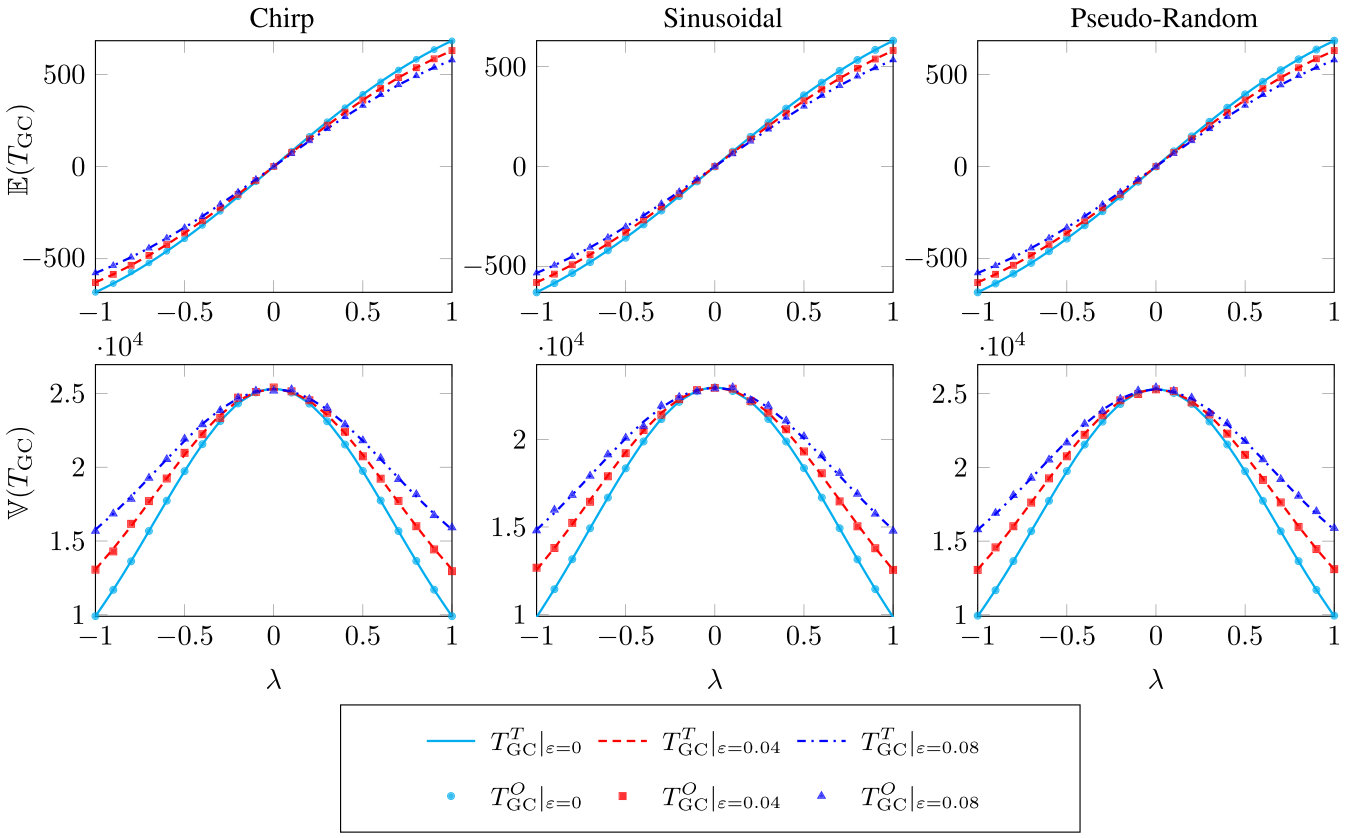

FIGURE 1. Verification of $\mathbb{E}(T_{\mathrm{GC}})$ in (32) and $\mathbb{V}(T_{\mathrm{GC}})$ in (33) established in Theorem 1 for $n = 50$ and $\varepsilon \in \{0, 0.04, 0.08\}$, respectively. The superscripts O and T stand for observed and theoretical values, respectively. Good agreements are observed between simulation results (markers) and theoretical counterparts (lines with different patterns). For comparison, the contamination-free versions (38) and (39) in Corollary 3 are also included in each subplot. The properties of odd (even) symmetry concerning $\mathbb{E}(T_{\mathrm{GC}})$ [$\mathbb{V}(T_{\mathrm{GC}})$] asserted in Corollary 1 can also be clearly observed.

$$\mathbb{V}(T_{\mathrm{SC}}) = \sum_{i=1}^{n} \left\{ 1 - (1-\varepsilon)^2 \left[2\Phi\left(\frac{\lambda y_1 + \mu_1}{\sigma_1} \right) - 1 \right]^2 \right\} y_i^2. \tag{55}$$

Proof: See Appendix H. □

B. ASYMPTOTIC RELATIVE EFFICIENCY IN NORMAL CASES

Corollary 7: Let $\{(X_i, y_i, Z_i)\}_{i=1}^n$ satisfy the data model presented in (1), where $\{Z_i\}_{i=1}^n$ are i.i.d. random variables following the normal distribution of $\mathcal{N}(\mu_1, \sigma_1^2)$. Then the Pitman ARE of T_{SC} to T_{MF} for weak signals ($\lambda \to 0$) is

$$\mathrm{ARE}_{\mathrm{SC,MF}} = \frac{\phi^2\left(\frac{\mu_1}{\sigma_1}\right)}{\Phi\left(\frac{\mu_1}{\sigma_1}\right) - \Phi^2\left(\frac{\mu_1}{\sigma_1}\right)} \tag{56}$$

Proof: From (54) and (55), it follows that

$$\mathbb{E}'(T_{\mathrm{SC}})\big|_{\substack{\varepsilon=0 \\ \lambda\to 0}} = \frac{2}{\sigma_1}\phi\left(\frac{\mu_1}{\sigma_1}\right) \sum_i y_i^2 \tag{57}$$

$$\mathbb{V}(T_{\mathrm{SC}})\big|_{\substack{\varepsilon=0 \\ \lambda\to 0}} = 4\left[\Phi\left(\frac{\mu_1}{\sigma_1}\right) - \Phi^2\left(\frac{\mu_1}{\sigma_1}\right)\right] \sum_i y_i^2 \tag{58}$$

Substituting (57), (58), (49) and (50) into (46) leads directly to (56). □

Remark 7: It is not difficult to verify that when $\mu_1 = 0$, (56) reaches its maximum, which is

$$\max \mathrm{ARE}_{\mathrm{SC,MF}} = \frac{2}{\pi}. \tag{59}$$

This result, compared with that of (53), explains the inferiority of SC to GC observed in the next section.

VI. NUMERICAL RESULTS

This section aims at 1) verifying the theoretical results established in in Theorem 1 and Theorem 2 by Monte Carlo simulations, 2) illustrating the advantages of GC in different scenarios, in terms of false alarm control, Pitman ARE and time-delay detection, compared with five frequently used detectors, namely, MFD, LO, SC, SR and KT. In the sequel, the notation $h = h_1(\Delta h)h_2$ trepresents a list of h starting from h_1 to h_2 with an increment of Δh.

A. EXPERIMENT SETTINGS

The parameters involved in (1) and (3) are as follows:

- the signal length $n \in \{50, 100, 150, 200\}$;
- $\lambda = -1(0.1)1$ in Figs. 1–2;
- $\varepsilon \in \{0, 0.04, 0.08\}$;
- $\mu_1 = 0$ and $\mu_2 = 0$;
- $\sigma_1 = 1$ and $\sigma_2 = 100$.

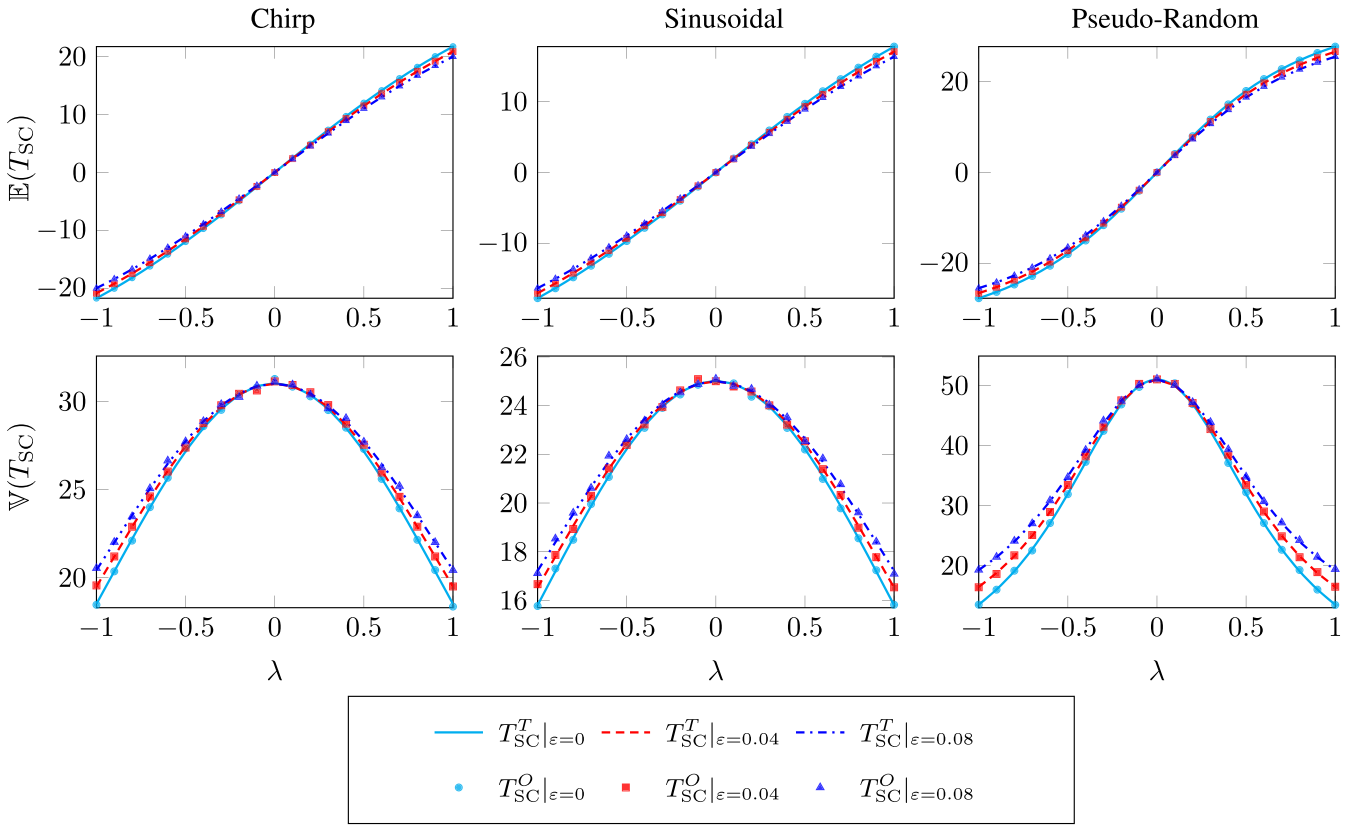

FIGURE 2. Verification of $\mathbb{E}(T_{\mathrm{SC}})$ in (54) and $\mathbb{V}(T_{\mathrm{SC}})$ in (55) established in Theorem 2 for $n = 50$ and $\varepsilon \in \{0, 0.04, 0.08\}$, respectively. Good agreements are observed between simulation results (markers) and theoretical counterparts (lines with different patterns).

Moreover, three prescribed signals $\{y_i\}_{i=1}^{n}$ are recruited in this study, as follows.

- Chirp signal with the following form

$$y_i = \begin{cases} \cos\left[\dfrac{1}{200}\left(2\pi f_0 \times i + \dfrac{F \times i^2}{200T}\right)\right] & \text{for } 0 \le i \le n; \\ 0 & \text{otherwise.} \end{cases} \tag{60}$$

  The associated parameters are set to be $f_0 = 0$, $T = 1$ and $F = 150$ in this work.
- Sinusoidal signal with the following form

$$y_i = \begin{cases} \sin\left[\dfrac{2\pi \times 5i}{200}\right] & \text{for } 0 \le i \le n; \\ 0 & \text{otherwise.} \end{cases} \tag{61}$$

- Pseudo-random signal formed by taking a segment of white Gaussian noise of length n.

The number of Monte Carlo trials is set to be 10^4 for purpose of accuracy. All noise samples are generated by functions in the Matlab `Statistics Toolbox`™.

B. VERIFICATION OF THEOREM 1 AND THEOREM 2

Fig. 1 verifies the correctness of (32) for $\mathbb{E}(T_{\mathrm{GC}})$ and (33) for $\mathbb{V}(T_{\mathrm{GC}})$ established in Theorem 1, by plotting the simulation results (markers of different shapes) as well as the corresponding theoretical results (lines of different patterns). Due to space limitation, we only present the results for $n = 50$ with respect to $\varepsilon \in \{0, 0.04, 0.08\}$. From left to right, the three columns of subplots correspond to the prescribed y-signals of chirp, sinusoidal, and pseudo-random type, respectively; whereas from top to bottom, the two rows of subplots correspond to theoretical and observed $\mathbb{E}(T_{\mathrm{GC}})$ and $\mathbb{V}(T_{\mathrm{GC}})$, respectively. Good agreements are observed between simulation results and theoretical counterparts. The property of odd (even) symmetry of $\mathbb{E}(T_{\mathrm{GC}})$ [$\mathbb{V}(T_{\mathrm{GC}})$] revealed in Corollary 1 can be clearly observed. Besides, it is seen that, with increase of ε, noticeable deviations of $\mathbb{V}(T_{\mathrm{GC}})$ from the contamination fee version (38) are observed, especially for $|\lambda|$ being large.

With the same layout as that in Fig 1, we present in Fig. 2 the simulation results (markers of different shapes) as well as theoretical counterparts concerning $\mathbb{E}(T_{\mathrm{SC}})$ and $\mathbb{V}(T_{\mathrm{SC}})$ established in Theorem 2, respectively. Good agreements are observed once more between the observed and theoretical results expressed in (54) and (55), respectively, illustrating the correctness of Theorem 2.

C. CONTROL OF FALSE ALARM PROBABILITIES FOR GC

As discussed in Remark 2, it is reasonable to approximate the null distribution of T_{GC} by a normal one with the form in (20)

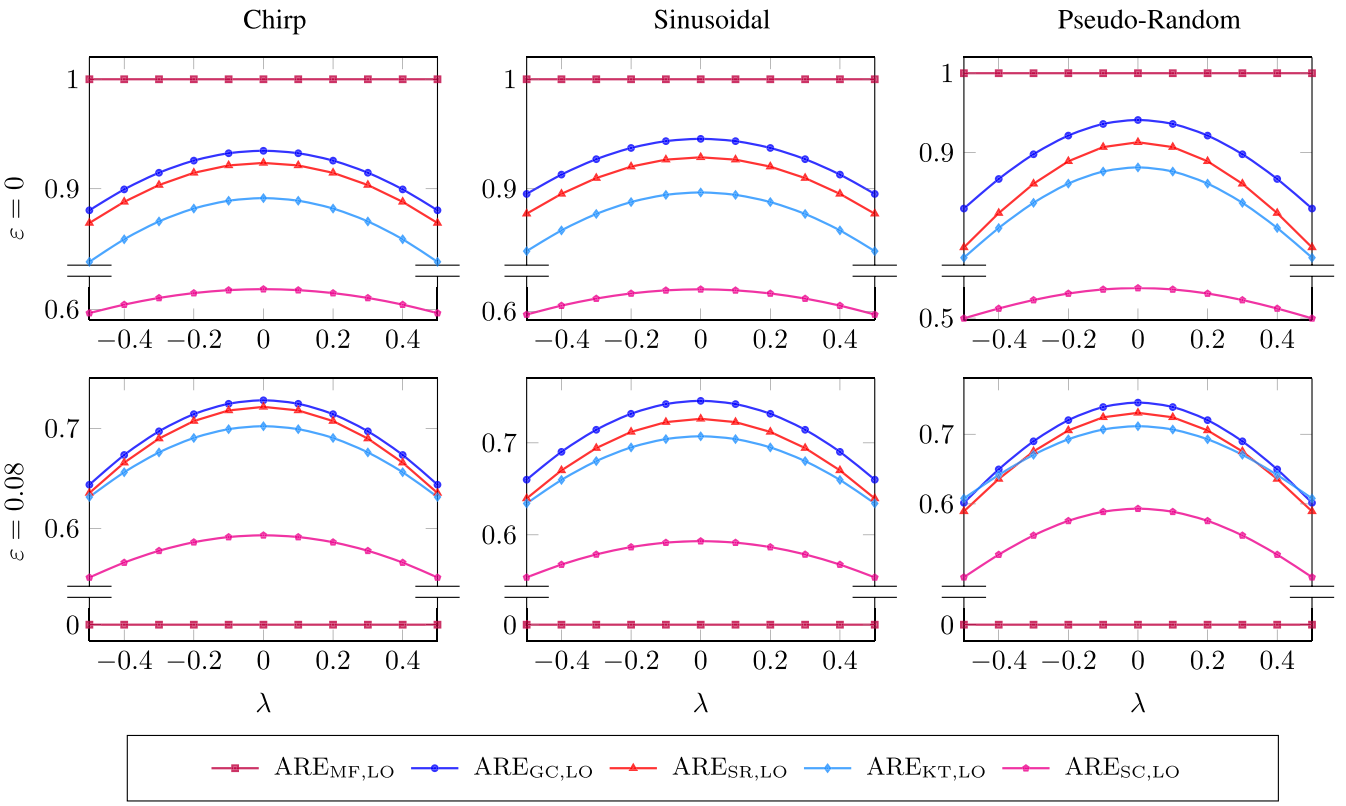

FIGURE 3. Comparison of ARE curves for $\lambda = -0.5(0.1)0.5$ and $n = 100$. From left to right, the three columns correspond to the prescribed y-signals of chirp, sinusoidal, and pseudo-random type, respectively; whereas from top to bottom, the two rows correspond to $\varepsilon = 0$ (normal cases) and $\varepsilon = 0.08$, respectively. From the top row, it is observed that, when the noise is strictly Gaussian, the ARE curves of T_{SC} are consistently lower than others, meaning the inferiority of SC to other detectors with higher ARE curves. From the bottom row, it is observed that, when $\varepsilon \neq 0$, the MFD, with zero ARE curves, performs the worst.

TABLE 1. Observed false alarm probabilities based on $\tilde{T}_{GC}$ defined in (62).

	Chirp				Sinusoidal				Pseudo-Random			
	$\alpha = 0.01$		$\alpha = 0.05$		$\alpha = 0.01$		$\alpha = 0.05$		$\alpha = 0.01$		$\alpha = 0.05$	
n	$P_{FA}(\alpha)$	$P_{FA}\left(\frac{\alpha}{2}\right)$	$P_{FA}(\alpha)$	$P_{FA}\left(\frac{\alpha}{2}\right)$	$P_{FA}(\alpha)$	$P_{FA}\left(\frac{\alpha}{2}\right)$	$P_{FA}(\alpha)$	$P_{FA}\left(\frac{\alpha}{2}\right)$	$P_{FA}(\alpha)$	$P_{FA}\left(\frac{\alpha}{2}\right)$	$P_{FA}(\alpha)$	$P_{FA}\left(\frac{\alpha}{2}\right)$
50	0.0100	0.0110	0.0507	0.0503	0.0103	0.0092	0.0527	0.0506	0.0093	0.0092	0.0511	0.0525
100	0.0098	0.0098	0.0517	0.0507	0.0108	0.0104	0.0522	0.0498	0.0108	0.0104	0.0491	0.0508
150	0.0094	0.0109	0.0511	0.0498	0.0106	0.0108	0.0513	0.0516	0.0105	0.0116	0.0493	0.0507
200	0.0107	0.0102	0.0508	0.0504	0.0107	0.0100	0.0510	0.0501	0.0111	0.0093	0.0505	0.0497

for n being large. Equivalently, we can employ a normalize version of T_{GC} as the detection statistic, that is,

$$\tilde{T}_{GC} \triangleq \frac{T_{GC} - \mathbb{E}(T_{GC})|_{\lambda=0}}{\sqrt{\mathbb{V}(T_{GC})|_{\lambda=0}}} \tag{62}$$

$$= \frac{T_{GC}}{\left\{\frac{n+1}{3}\left[n\sum y_i^2 - \left(\sum y_i\right)^2\right]\right\}^{\frac{1}{2}}} \tag{63}$$

to control the false alarm probabilities more conveniently, since, as n large, $\tilde{T}_{GC}$ converges in distribution to $\mathcal{N}(0, 1)$ approximately in the null case. Then, given the false alarm probability α to be controlled, the corresponding threshold η_α for unilateral test $\lambda = 0$ vs. $\lambda > 0$, or $\eta_{\frac{\alpha}{2}}$ for bilateral test $\lambda = 0$ vs. $\lambda \neq 0$ can be determined via

$$\eta_\alpha = \Phi^{-1}(1 - \alpha) \tag{64}$$

and

$$\eta_{\frac{\alpha}{2}} = \Phi^{-1}\left(1 - \frac{\alpha}{2}\right) \tag{65}$$

respectively, where $\Phi^{-1}(\cdot)$ stands for the inverse cdf of $\mathcal{N}(0, 1)$.

Table 1 lists the observed false alarm probabilities based on $\tilde{T}_{GC}$ for $\alpha = 0.01$ and $\alpha = 0.05$ with respect to three prescribed y signals with $n = 50, 100, 150, 200$. Note that in

TABLE 2. Performance comparison for time-delay estimation.

	$\varepsilon = 0$						$\varepsilon = 0.04$					
λ	$T_{\rm LO}$	$T_{\rm MF}$	$T_{\rm GC}$	$T_{\rm SR}$	$T_{\rm KT}$	$T_{\rm SC}$	$T_{\rm LO}$	$T_{\rm MF}$	$T_{\rm GC}$	$T_{\rm SR}$	$T_{\rm KT}$	$T_{\rm SC}$
0.1	800±0.2	800±0.2	800±0.3	800±0.3	800±0.4	800±0.5	798±169.4	801±479.8	800±204.0	800±204.4	799±205.0	802±266.6
0.2	800±0	800±0	800±0	800±0.1	800±0.1	800±0.3	800±10.2	792±475.8	800±15.3	800±15.6	800±15.7	800±31.0
0.3	800±0	800±0	800±0	800±0	800±0	800±0.2	800±1.8	804±473.6	800±3.6	800±4.3	800±4.2	800±6.1
0.4	800±0	800±0	800±0	800±0	800±0	800±0.1	800±0.7	806±462.2	800±1.3	800±1.5	800±1.4	800±1.6
0.5	800±0	800±0	800±0	800±0	800±0	800±0.1	800±0.6	794±460.9	800±0.7	800±1.0	800±0.8	800±1.0

Table 1,

$$P_{\rm FA}(\alpha) \triangleq \Pr(\tilde{T}_{\rm GC} > \alpha)$$
$$P_{\rm FA}\left(\frac{\alpha}{2}\right) \triangleq \Pr\left(|\tilde{T}_{\rm GC}| > \frac{\alpha}{2}\right).$$

It is seen that the observed false alarm probabilities agree well the corresponding nominal values for all $n \geq 50$ and all three types of the prescribed signals. It is thus safe to approximate the null distribution of $\tilde{T}_{\rm GC}$ by $\mathcal{N}(0, 1)$ in practice for $n \geq 50$.

D. COMPARISON OF PITMAN ARE

Fig. 3 compares the Pitman ARE of $T_{\rm GC}$ and other four detectors to $T_{\rm LO}$, based on (46) and (47), corresponding to three known signals for $n = 100$, $\lambda = -0.5(0.1)0.5$, $\varepsilon = 0$ and $\varepsilon = 0.08$, respectively. Since, from (6) and (7), the mean and variance of $T_{\rm LO}$ have no closed forms under the CGM of (3), the efficacy of $T_{\rm LO}$ in (46) and (47) are computed by numerical integration and numerical differentiation.

It is observed in Fig. 3 that, when $\varepsilon = 0$ (top row), 1) $T_{\rm SC}$, whose ARE curves are lower than all of the others, performs the worst, 2) $T_{\rm MF}$ has the highest ARE curves (equaling to 1), outperforms the other detectors, 3) the ARE curves of $T_{\rm SR}$ are higher than $T_{\rm KT}$, which means that $T_{\rm SR}$ is more efficient than $T_{\rm KT}$ when signal is weak, 4) when $\varepsilon = 0.08$ (bottom row), the ARE curves of $T_{\rm GC}$ lie in between those of $T_{\rm MF}$ and $T_{\rm SR}$ ($T_{\rm KT}$), manifesting its superiority over $T_{\rm SR}$ and $T_{\rm KT}$;, 5) $T_{\rm MF}$, whose ARE curves (around 0) are significantly lower than those of others, performs the worst, 6) the ARE curves of $T_{\rm GC}$ are the highest, manifesting again its superiority over $T_{\rm SR}$ and $T_{\rm KT}$, and 7) $T_{\rm SC}$ underperforms other detectors except for $T_{\rm MF}$. The results in Fig. 3 allow us to order the performance, in terms of Pitman ARE, as

$$\begin{aligned} T_{\rm SC} < T_{\rm KT} < T_{\rm SR} < T_{\rm GC} < T_{\rm LO} = T_{\rm MF} \quad &\text{for } \varepsilon = 0 \\ T_{\rm MF} < T_{\rm SC} < T_{\rm KT} < T_{\rm SR} < T_{\rm GC} < T_{\rm LO} \quad &\text{for } \varepsilon > 0 \end{aligned} \tag{66}$$

when the signal strength is weak.

E. EXAMPLE OF TIME-DELAY ESTIMATION

To further demonstrate the usefulness of the proposed Gini correlator, we provide an example of time-delay estimation, which is customary in signal processing. The problem is formulated by modifying (1) into

$$X[i] = \lambda y[i - \tau_0] + Z[i], \quad -\infty < i < \infty \tag{67}$$

where τ_0 is the time-delay to be estimated, and $Z[i]$ obeys the CGM model (3) with $\varepsilon = 0$ and $\varepsilon = 0.04$, respectively.

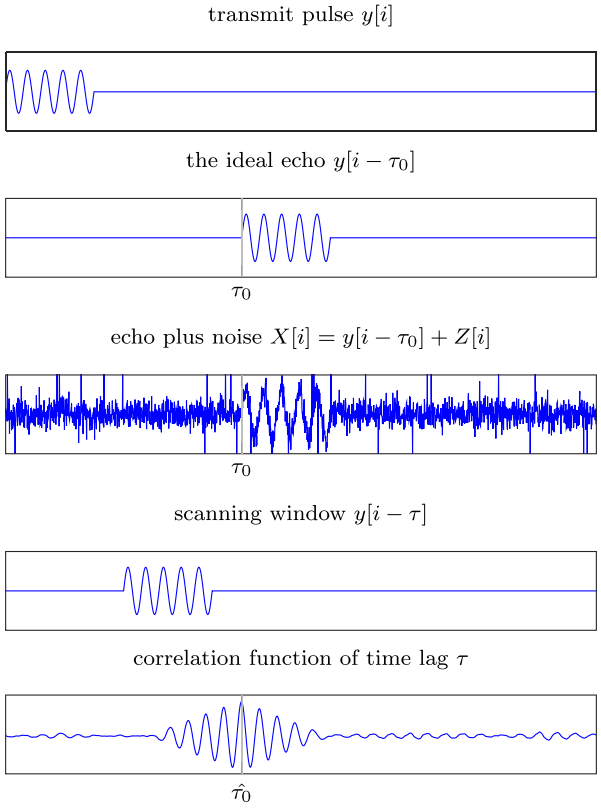

FIGURE 4. Schematic illustration of estimating the time-delay τ_0. In the bottom panel, the time-shift $\hat{\tau}_0$ corresponding to the maximum of the correlation function is considered as an estimate of the true time-delay τ_0.

As illustrated in Fig. 4, the procedure of estimating τ_0 is to firstly generate a correlation function with $T_{\rm LO}$, $T_{\rm MF}$, $T_{\rm GC}$, $T_{\rm SR}$, $T_{\rm KT}$ and $T_{\rm SC}$, by correlating the scanning window of $\{y[i - \tau]\}_{i=1}^{n}$ between the received signal $X[i]$ with respect to τ. The time-shift $\hat{\tau}_0$ corresponding to the maximum of the correlation function is then restored as an estimate of τ_0. In this example we set the real time-delay $\tau_0 = 800$.

Table 2 lists the estimation results of time-delay, in terms of $\overline{\hat{\tau}_0} \pm$ std. It is seen that, for $\varepsilon = 0$ (the noise being pure Gaussian), all detectors performs comparably well. However, when the noise is corrupted with a tiny fraction of impulsive component ($\varepsilon = 0.04$), $T_{\rm MF}$ loses completely the detection power, irrespective of the magnitudes of SNR. On the other hand, $T_{\rm LO}$, $T_{\rm GC}$, $T_{\rm SR}$, $T_{\rm KT}$ and $T_{\rm SC}$ performs well in this case, in the sense of producing accurate estimates of τ_0 with no

bias and small standard deviations. Specifically, the results in Table 2 show the following order of performance, in terms of time-delay estimation, as

$$\begin{aligned} T_{\mathrm{SC}} &< T_{\mathrm{KT}} \sim T_{\mathrm{SR}} \sim T_{\mathrm{GC}} \sim T_{\mathrm{LO}} = T_{\mathrm{MF}} \quad \text{for } \varepsilon = 0 \\ T_{\mathrm{MF}} &\ll T_{\mathrm{SC}} < T_{\mathrm{KT}} \sim T_{\mathrm{SR}} < T_{\mathrm{GC}} < T_{\mathrm{LO}} \quad \text{for } \varepsilon > 0 \end{aligned} \tag{68}$$

VII. CONCLUSION

In this paper, we proposed a nonparametric detector, called Gini correlator (GC), to deal with the problem of detecting the presence/absence of known signals buried in impulsive noise. Based on a specified contaminate Gaussian model CGM simulating reasonably the impulsive noise that frequently encountered in practice, we established the analytic formulas concerning the expectation and variance of GC. These novel theoretical results with extensive Monte Carlo simulations suggest that

- in the null case, the mean and variance of GC depend only on the prescribed known signals, which allows us to accurately control the false alarm probability with the assistance of the central limit theorem;
- GC performs comparably well with the matched filter based detector (MFD) [and also the locally optimal detector (LOD)] when the noise is i.i.d. Gaussian, in the sense of ARE being as high as $3/\pi$;
- GC is robust against the impulsive noise, in the sense that its mean and variance are only slightly affected by the magnitude of the fraction of impulsive component;
- GC performs better than SR and KT, in terms of ARE analysis as well as time-delay estimation.

Based on the comparative studies, it appears that in most cases, GC is not optimal, but it is always the second best. In other words, GC bridges the gap between LO and SR (KT). This feature of sub-optimality at least avoids the worst consequences when no prior knowledge as to whether or not impulsivity exists in noise. The mathematical tractability, easy implementation and empirical findings revealed in this work might shed new light on the topic of known signal detection, which is widely applied in the area of statistical processing.

APPENDIX A
PROOF OF LEMMA 1

Proof: Substituting the relationship $P_i = \sum_{j\neq i}^{n} H(X_i - X_j) + 1$ [46] into (4), it follows that

$$\begin{aligned} T_{\mathrm{GC}} &= \sum_{i=1}^{n} (2P_i - 1 - n) y_i \\ &= \sum_{i=1}^{n} \left\{ 2\Big[\sum_{j\neq i=1}^{n} H(X_i - X_j) + 1 \Big] - 1 - n \right\} y_i \\ &= 2 \sum_{i\neq j=1}^{n}\sum^{n} H(X_i - X_j) y_i + (1-n) \sum_{i=1}^{n} y_i. \end{aligned} \tag{69}$$

Reversing the roles of the subsripts i and j in (69) yields Substituting the subscripts i and j

$$T_{\mathrm{GC}} = 2 \sum_{i\neq j=1}^{n}\sum^{n} H(X_j - X_i) y_j + (1-n) \sum_{j=1}^{n} y_j. \tag{70}$$

Summing up (69) and (70) and using the result

$$H(X_i - X_j) = 1 - H(X_j - X_i), \tag{71}$$

we obtain

$$\begin{aligned} 2T_{\mathrm{GC}} = {} & 2 \sum_{i\neq j}^{n}\sum_{j=1}^{n} H(X_i - X_j) y_i + (1-n) \sum_{i=1}^{n} y_i \\ & - 2 \sum_{i\neq j}^{n}\sum_{i=1}^{n} H(X_i - X_j) y_j - (1-n) \sum_{i=1}^{n} y_j \end{aligned} \tag{72}$$

which means that

$$\begin{aligned} T_{\mathrm{GC}} &= \sum_{i\neq j=1}^{n}\sum^{n} H(X_i - X_j) y_i - \sum_{i\neq j=1}^{n}\sum^{n} H(X_i - X_j) y_j \\ &= \sum_{i\neq j=1}^{n}\sum^{n} H(X_i - X_j)(y_i - y_j) \end{aligned} \tag{73}$$

hence the result. □

APPENDIX B
PROOF OF LEMMA 2

Proof: From (11) in Lemma 1 and the abbreviations (12) and (13), it follows that

$$T_{\mathrm{GC}} = \sum_{i\neq j=1}^{n}\sum^{n} H_{ij} \Delta_{ij} \tag{74}$$

which leads to (14) directly after taking expectation.

Substituting (74) into the right side of the following formula

$$\mathbb{V}(T_{\mathrm{GC}}) = \mathbb{C}(T_{\mathrm{GC}}, T_{\mathrm{GC}})$$

we have

$$\begin{aligned} \mathbb{V}(T_{\mathrm{GC}}) &= \mathbb{C}\left(\sum_{i\neq j=1}^{n}\sum^{n} H_{ij}\Delta_{ij}, \sum_{k\neq l=1}^{n}\sum^{n} H_{kl}\Delta_{kl} \right) \\ &= \sum_{i\neq j=1}^{n}\sum^{n}\sum_{k\neq l=1}^{n}\sum^{n} \mathbb{C}(H_{ij}, H_{kl}) \Delta_{ij}\Delta_{kl} \qquad (75) \\ &= \sum_{i\neq j=1}^{n}\sum^{n} \underbrace{\mathbb{C}(H_{ij}, H_{ij})}_{=\mathbb{V}(H_{ij})} \Delta_{ij}^2 \qquad (76) \\ &\quad + \sum_{i\neq j=1}^{n}\sum^{n} \mathbb{C}(H_{ij}, H_{ji}) \Delta_{ij}\Delta_{ji} \qquad (77) \\ &\quad + \sum_{i\neq j\neq k=1}^{n}\sum^{n}\sum^{n} \mathbb{C}(H_{ij}, H_{ik}) \Delta_{ij}\Delta_{ik} \qquad (78) \end{aligned}$$

$$+\sum_{i\neq j\neq k=1}^{n}\sum^{n}\sum^{n}\mathbb{C}(H_{ij},H_{ki})\Delta_{ij}\Delta_{ki} \tag{79}$$

$$+\sum_{i\neq j\neq k=1}^{n}\sum^{n}\sum^{n}\mathbb{C}(H_{ij},H_{jk})\Delta_{ij}\Delta_{jk} \tag{80}$$

$$+\sum_{i\neq j\neq k=1}^{n}\sum^{n}\sum^{n}\mathbb{C}(H_{ij},H_{kj})\Delta_{ij}\Delta_{kj} \tag{81}$$

$$+\sum_{i\neq j\neq k\neq l=1}^{n}\sum^{n}\sum^{n}\sum^{n}\underbrace{\mathbb{C}(H_{ij},H_{kl})}_{=0}\Delta_{ij}\Delta_{kl} \tag{82}$$

$$=S_1+S_2+S_3+S_4+S_5+S_6+S_7 \text{ (say.)} \tag{83}$$

Applying the result $H_{ji}=1-H_{ij}$, it follows that

$$\mathbb{C}(H_{ij},H_{ji})=\mathbb{C}(H_{ij},1-H_{ij})=-\mathbb{C}(H_{ij},H_{ij}) \tag{84}$$

Substituting this result into (77) and noting $\Delta_{ji}=-\Delta_{ij}$, we have that the double summation S_2 in (77) is equal to S_1 in (76). In a similar manner, we also have $S_3=S_4$ and $S_5=S_6$. Now we show that $S_5=S_3$. Employing (84) once more, it follows that

$$S_5=\sum_{i\neq j\neq k=1}^{n}\sum^{n}\sum^{n}\mathbb{C}(H_{ij},H_{jk})\Delta_{ij}\Delta_{jk} \tag{85}$$

$$=\sum_{i\neq j\neq k=1}^{n}\sum^{n}\sum^{n}\mathbb{C}(1-H_{ji},H_{jk})\Delta_{ij}\Delta_{jk} \tag{86}$$

$$=\sum_{i\neq j\neq k=1}^{n}\sum^{n}\sum^{n}\mathbb{C}(H_{ji},H_{jk})\Delta_{ji}\Delta_{jk}=S_3. \tag{87}$$

Therefore,

$$\mathbb{V}(T_{\mathrm{GC}})=2S_1+4S_3 \tag{88}$$

which is (15) and hence the lemma holds true. □

APPENDIX C
PROOF OF LEMMA 3

Proof: Denote by $F_Z(z)$ the cumulative distribution function (cdf) of Z. When $\lambda=0$ in (1), we have $H_{ij}=H(Z_i-Z_j)$. Applying the i.i.d. assumption of $\{Z_i\}_{i=1}^n$, we have

$$\begin{aligned}\mathbb{E}(H_{ij})&=\int_{-\infty}^{\infty}\int_{-\infty}^{\infty}H(z_i-z_j)dF_Z(z_i)dF_Z(z_j)\\&=\int_{-\infty}^{\infty}\int_{-\infty}^{z_i}dF_Z(z_j)dF_Z(z_i)\\&=\int_{-\infty}^{\infty}F_Z(z_i)dF_Z(z_i)=\int_0^1 t\,dt=\frac{1}{2},\end{aligned} \tag{89}$$

$$\begin{aligned}\mathbb{E}(H_{ij}^2)&=\mathbb{E}(H_{ij})=\frac{1}{2},\\\mathbb{V}(H_{ij})&=\mathbb{E}(H_{ij}^2)-\mathbb{E}^2(H_{ij})=\frac{1}{4},\\\mathbb{E}(H_{ij}H_{ik})&=\int_{-\infty}^{\infty}\int_{-\infty}^{z_i}\int_{-\infty}^{z_i}dF_Z(z_i)dF_Z(z_j)dF_Z(z_k)\\&=\int_{-\infty}^{\infty}F_Z^2(z_i)dF_Z(z_i)=\int_0^1 t^2\,dt=\frac{1}{3},\end{aligned} \tag{90}$$

and hence

$$\mathbb{C}(H_{ij},H_{ik})=\underbrace{\mathbb{E}(H_{ij}H_{ik})}_{1/3}-\underbrace{\mathbb{E}(H_{ij})\mathbb{E}(H_{ik})}_{1/4}=\frac{1}{12}. \tag{91}$$

Substituting (89) into (14) produces

$$\mathbb{E}(T_{\mathrm{GC}})=\frac{1}{2}\sum_{i\neq j=1}^{n}\sum^{n}(y_i-y_j)=0 \tag{92}$$

which is (16).

Plugging the results (90) and (91) into (15) leads readily to

$$\mathbb{V}(T_{\mathrm{GC}})=\underbrace{\frac{1}{2}\sum_{i\neq j=1}^{n}\sum^{n}(y_i-y_j)^2}_{\triangleq V_1} \tag{93}$$

$$+\underbrace{\frac{1}{3}\sum_{i\neq j\neq k=1}^{n}\sum^{n}\sum^{n}(y_i-y_j)(y_i-y_j)}_{\triangleq V_2} \tag{94}$$

which is compatible with (18). It also follows that

$$\begin{aligned}V_1&=\sum_{i\neq j=1}^{n}\sum^{n}(y_i-y_j)^2=\sum_{i=1}^{n}\sum_{j=1}^{n}(y_i^2-2y_iy_j+y_j^2)\\&=2n\sum_{i=1}^{n}y_i^2-2\left(\sum_{i=1}^{n}y_i\right)^2,\end{aligned} \tag{95}$$

and

$$\begin{aligned}V_2&=\sum_{i\neq j\neq k=1}^{n}\sum^{n}\sum^{n}(y_i-y_j)(y_i-y_k)\\&=\underbrace{\sum_{i=1}^{n}\sum_{j=1}^{n}\sum_{k=1}^{n}(y_i-y_j)(y_i-y_k)}_{\triangleq V_3}-\sum_{i\neq j=1}^{n}\sum^{n}(y_i-y_j)^2\end{aligned} \tag{96}$$

where

$$\begin{aligned}V_3&=\sum_{i=1}^{n}\sum_{j=1}^{n}\sum_{k=1}^{n}(y_i^2-y_iy_k-y_iy_j+y_jy_k)\\&=n^2\sum_{i=1}^{n}y_i^2-n\left(\sum_{i=1}^{n}y_i\right)^2=\frac{n}{2}V_1.\end{aligned} \tag{97}$$

A combination of (93)–(97) gives

$$\mathbb{V}(T_{\mathrm{GC}})=\frac{1}{2}V_1+\frac{1}{3}(V_3-V_1)=\frac{n+1}{6}\sum_{i\neq j=1}^{n}\sum^{n}(y_i-y_j)^2 \tag{98}$$

which is the form in (18) and becomes the form in (19) upon substitution of (95) into (98). □

APPENDIX D
PROOF OF LEMMA 4

Proof: Let

$$\Delta\xi'_{12} \triangleq \frac{\Delta\xi_{12}-\Delta\nu_{12}}{\varsigma_{12}}$$
$$\Delta\xi'_{13} \triangleq \frac{\Delta\xi_{13}-\Delta\nu_{13}}{\varsigma_{13}}$$

Then, from the normal assumption, we have

$$(\Delta\xi'_{12},\Delta\xi'_{12}) \sim \mathcal{N}\left(0,0,1,1,\frac{\varsigma_1^2}{\varsigma_{12}\varsigma_{13}}\right). \tag{99}$$

Therefore,

$$\begin{aligned}\mathbb{E}[H(\Delta\xi_{12})] &= \mathbb{E}\left[H\left(\frac{\Delta\xi_{12}}{\varsigma_{12}}\right)\right] = \Pr\left(\frac{\Delta\xi_{12}}{\varsigma_{12}}>0\right)\\ &= \Pr\left(\Delta\xi'_{12}>-\frac{\Delta\nu_{12}}{\varsigma_{12}}\right)\\ &= \Pr\left(\Delta\xi'_{12}<\frac{\Delta\nu_{12}}{\varsigma_{12}}\right) = \Phi\left(\frac{\Delta\nu_{12}}{\varsigma_{12}}\right)\end{aligned}$$

which is (21). Moreover,

$$\begin{aligned}&\mathbb{E}[H(\Delta\xi_{12})H(\Delta\xi_{13})]\\ &= \mathbb{E}\left[H\left(\frac{\Delta\xi_{12}}{\varsigma_{12}}\right)H\left(\frac{\Delta\xi_{13}}{\varsigma_{13}}\right)\right]\\ &= \Pr\left(\frac{\Delta\xi_{12}}{\varsigma_{12}}>0,\frac{\Delta\xi_{13}}{\varsigma_{13}}>0\right)\\ &= \Pr\left(\Delta\xi'_{12}>-\frac{\Delta\nu_{12}}{\varsigma_{12}},\Delta\xi'_{13}>-\frac{\Delta\nu_{13}}{\varsigma_{13}}\right)\\ &= \Pr\left(\Delta\xi'_{12}<\frac{\Delta\nu_{12}}{\varsigma_{12}},\Delta\xi'_{13}<\frac{\Delta\nu_{13}}{\varsigma_{13}}\right)\\ &= \Psi\left(\frac{\Delta\nu_{12}}{\varsigma_{12}},\frac{\Delta\nu_{12}}{\varsigma_{12}},\frac{\varsigma_1^2}{\varsigma_{12}\varsigma_{13}}\right)\end{aligned}$$

which completes the proof of (22). □

APPENDIX E
PROOF OF LEMMA 5

Proof: Substituting (1) into (5) and taking expectation on both sides, we have

$$\begin{aligned}\mathbb{E}(T_{\mathrm{MF}}) &= \mathbb{E}\left[\sum(\lambda y_i+Z_i)y_i\right]\\ &= \lambda\sum y_i^2+\sum\mathbb{E}(Z_i)y_i = \lambda\sum y_i^2+\mu_Z\sum y_i\end{aligned}$$

which is the first lemma statement (23).

By definition,

$$\begin{aligned}\mathbb{V}(T_{\mathrm{MF}}) &= \mathbb{C}(T_{\mathrm{MF}},T_{\mathrm{MF}})\\ &= \mathbb{C}\left[\sum_{i=1}^n(\lambda y_i+Z_i)y_i,\sum_{j=1}^n(\lambda y_j+Z_j)y_j\right]\\ &= \sum_{i=1}^n\sum_{j=1}^n y_iy_j\mathbb{C}\left[(\lambda y_i+Z_i),(\lambda y_j+Z_j)\right]\\ &= \sum_{i=1}^n\sum_{j=1}^n y_iy_j\mathbb{C}(Z_i,Z_j)\\ &= \sum_{i=1}^n y_i^2\mathbb{V}(Z_i)+\sum_{i\neq j=1}^n\sum^n y_iy_j\underbrace{\mathbb{C}(Z_i,Z_j)}_{=0}\\ &= \sigma_Z^2\sum_{i=1}^n y_i^2\end{aligned}$$

which is the second lemma statement (24). □

APPENDIX F
PROOF OF THEOREM 1

Proof: We first deal with $\mathbb{E}(T_{\mathrm{GC}})$. Based on Model (3), it follows that the joint pdf of (X_i,X_j) is

$$\begin{aligned}&\varphi_{ij}(x_i,x_j)\\ &= [(1-\varepsilon)\phi_i(x_i)+\varepsilon\psi_i(x_i)][(1-\varepsilon)\phi_j(x_j)+\varepsilon\psi_j(x_j)]\\ &= (1-\varepsilon)^2\phi_i\phi_j+\varepsilon(1-\varepsilon)\phi_i\psi_j+\varepsilon(1-\varepsilon)\phi_j\psi_i+\varepsilon^2\psi_i\psi_j.\end{aligned} \tag{100}$$

Then,

$$\begin{aligned}\mathbb{E}(H_{ij}) &= \int_{-\infty}^{\infty}\int_{-\infty}^{\infty}H(x_i-x_j)\varphi_{ij}(x_i,x_j)dx_idx_j\\ &= (1-\varepsilon)^2E_1+\varepsilon(1-\varepsilon)E_2+\varepsilon(1-\varepsilon)E_3+\varepsilon^2E_4\end{aligned} \tag{101}$$

where $E_1,\ldots,E_4$ are expectation terms of H_{ij} with respect to four pdfs in (100). Resorting to the first statement (21) in Lemma 4, we have

$$E_1 = \Phi\left[\frac{\lambda(y_i-y_j)}{\sqrt{2}\sigma_1}\right](=\Phi_{ij}) \tag{102}$$

by noticing that, in this case, $\Delta\xi_{ij}=X_i-X_j$, $\nu_1=\lambda y_i+\mu_1$, $\nu_2=\lambda y_j+\mu_1$, $\varsigma_1^2=\sigma_1^2$ and $\varsigma_2^2=\sigma_1^2$. Similarly, we also have

$$E_2 = \Phi\left(\frac{\lambda\Delta_{ij}+\Delta\mu}{\sqrt{\sigma_1^2+\sigma_2^2}}\right)\to\underbrace{\Phi(0)=\frac{1}{2}}_{\text{as }\sigma_2\to\infty} \tag{103}$$

$$E_3 = \Phi\left(\frac{\lambda\Delta_{ij}-\Delta\mu}{\sqrt{\sigma_1^2+\sigma_2^2}}\right)\to\underbrace{\Phi(0)=\frac{1}{2}}_{\text{as }\sigma_2\to\infty} \tag{104}$$

$$E_4 = \Phi\left(\frac{\lambda\Delta_{ij}}{\sqrt{2}\sigma_2}\right)\to\underbrace{\Phi(0)=\frac{1}{2}}_{\text{as }\sigma_2\to\infty}. \tag{105}$$

Substituting (102)–(105) into (101) produces

$$\mathbb{E}(H_{ij}) = (1-\varepsilon)^2\Phi_{ij}+\varepsilon\left(1-\frac{\varepsilon}{2}\right) \tag{106}$$

which, with the assistance of (14) in Lemma 2, leads to

$$\begin{aligned}\mathbb{E}(T_{\mathrm{GC}}) &= \sum_{i\neq j=1}^{n}\sum^{n}\mathbb{E}(H_{ij})\Delta_{ij}\\ &= \underbrace{(1-\varepsilon)^2\sum_{i\neq j=1}^{n}\sum^{n}\Phi_{ij}\Delta_{ij}}_{\text{the result of (32)}} + \varepsilon\left(1-\tfrac{\varepsilon}{2}\right)\underbrace{\sum_{i\neq j=1}^{n}\sum^{n}\Delta_{ij}}_{=0}\end{aligned}$$

In a similar way, we can also obtain

$$\mathbb{E}(H_{ik}) = (1-\varepsilon)^2\Phi_{ik} + \varepsilon\left(1-\frac{\varepsilon}{2}\right). \tag{107}$$

To evaluate $\mathbb{V}(T_{\mathrm{GC}})$, it suffices to work out $\mathbb{V}(H_{ij})$ and $\mathbb{C}(H_{ij}, H_{ik})$, which are required in Lemma 2. Since $H^2(\cdot) = H(\cdot)$, we have

$$\mathbb{V}(H_{ij}) = \mathbb{E}(H_{ij}^2) - \mathbb{E}^2(H_{ij}) = \mathbb{E}(H_{ij}) - \mathbb{E}^2(H_{ij}). \tag{108}$$

Substituting (106) into (108) and tidying up, it follows that

$$\mathbb{V}(H_{ij}) = (1-\varepsilon)^4\Phi_{ij}(1-\Phi_{ij}) + \frac{1}{4}[1-(1-\varepsilon)^4]. \tag{109}$$

By definition,

$$\mathbb{C}(H_{ij}, H_{ik}) = \mathbb{E}(H_{ij}H_{ik}) - \mathbb{E}(H_{ij})\mathbb{E}(H_{ik}) \tag{110}$$

where only the first term on the right side needs to be worked out. Denote by $\varphi_{ijk}(x_i, x_j, x_k)$ the joint pdf of (X_i, X_j, X_k). We have, from Model (3),

$$\begin{aligned}&\varphi_{ijk}\\ &= \Pi_{\ell\in\{i,j,k\}}[(1-\varepsilon)\phi_\ell(x_\ell) + \varepsilon\psi_\ell(x_\ell)]\\ &= (1-\varepsilon)^3\phi_i\phi_j\phi_k + \varepsilon^3\psi_i\psi_j\psi_k\\ &\quad + \varepsilon(1-\varepsilon)^2\phi_i\phi_j\psi_k + \varepsilon(1-\varepsilon)^2\phi_i\psi_j\phi_k + \varepsilon(1-\varepsilon)^2\psi_i\phi_j\phi_k\\ &\quad + \varepsilon^2(1-\varepsilon)\phi_i\psi_j\psi_k + \varepsilon^2(1-\varepsilon)\psi_i\phi_j\psi_k + \varepsilon^2(1-\varepsilon)\psi_i\psi_j\phi_k.\end{aligned} \tag{111}$$

Hence,

$$\begin{aligned}\mathbb{E}(H_{ij}H_{ik}) &= \iiint_{-\infty}^{+\infty} H(x_i-x_j)H(x_i-x_k)\varphi_{ijk}\,dx_i dx_j dx_k\\ &= (1-\varepsilon)^3 M_1 + \varepsilon^3 M_2\\ &= \varepsilon(1-\varepsilon)^2(M_3+M_4+M_5)\\ &\quad + \varepsilon^2(1-\varepsilon)(M_6+M_7+M_8)\end{aligned} \tag{112}$$

where, along with the result (22) in Lemma 4,

$$\begin{aligned}M_1 &= \iiint_{-\infty}^{\infty} H(x_i-x_j)H(x_i-x_k)\phi_i\phi_j\phi_k\,dx_i dx_j dx_k\\ &= \Psi\left(\frac{\lambda\Delta_{ij}}{\sqrt{2}\sigma_1}, \frac{\lambda\Delta_{ik}}{\sqrt{2}\sigma_1}, \frac{1}{2}\right) (= \Psi_{ijk})\end{aligned} \tag{113}$$

$$\begin{aligned}M_2 &= \iiint_{-\infty}^{\infty} H(x_i-x_j)H(x_i-x_k)\psi_i\psi_j\psi_k\,dx_i dx_j dx_k\\ &= \Psi\left(\frac{\lambda\Delta_{ij}}{\sqrt{2}\sigma_2}, \frac{\lambda\Delta_{ik}}{\sqrt{2}\sigma_2}, \frac{1}{2}\right) \underbrace{\to \Psi\left(0, 0, \frac{1}{2}\right)}_{\text{as } \varsigma_2\to\infty} = \frac{1}{3}\end{aligned} \tag{114}$$

$$\begin{aligned}M_3 &= \iiint_{-\infty}^{\infty} H(x_i-x_j)H(x_i-x_k)\phi_i\phi_j\psi_k\,dx_i dx_j dx_k\\ &= \Psi\left(\frac{\lambda\Delta_{ij}}{\sqrt{2}\sigma_1}, \frac{\lambda\Delta_{ik}+\Delta\mu}{\sqrt{\sigma_1^2+\sigma_2^2}}, \frac{\sigma_1}{\sqrt{2}\sqrt{\sigma_1^2+\sigma_2^2}}\right)\\ &\quad \underbrace{\to \Psi\left(\frac{\lambda\Delta_{ij}}{\sqrt{2}\sigma_1}, 0, 0\right)}_{\text{as } \varsigma_2\to\infty} = \Phi\left(\frac{\lambda\Delta_{ij}}{\sqrt{2}\sigma_1}\right)\Phi(0) = \frac{1}{2}\Phi_{ij}\end{aligned} \tag{115}$$

$$\begin{aligned}M_4 &= \iiint_{-\infty}^{\infty} H(x_i-x_j)H(x_i-x_k)\phi_i\psi_j\phi_k\,dx_i dx_j dx_k\\ &= \Psi\left(\frac{\lambda\Delta_{ij}+\Delta\mu}{\sqrt{\sigma_1^2+\sigma_2^2}}, \frac{\lambda\Delta_{ik}}{\sqrt{2}\sigma_1}, \frac{\sigma_1}{\sqrt{2}\sqrt{\sigma_1^2+\sigma_2^2}}\right)\\ &\quad \underbrace{\to \Psi\left(0, \frac{\lambda\Delta_{ik}}{\sqrt{2}\sigma_1}, 0\right)}_{\text{as } \varsigma_2\to\infty} = \Phi\left(\frac{\lambda\Delta_{ik}}{\sqrt{2}\sigma_1}\right)\Phi(0) = \frac{1}{2}\Phi_{ik}\end{aligned} \tag{116}$$

$$\begin{aligned}M_5 &= \iiint_{-\infty}^{\infty} H(x_i-x_j)H(x_i-x_k)\psi_i\phi_j\phi_k\,dx_i dx_j dx_k\\ &= \Psi\left(\frac{\lambda\Delta_{ij}-\Delta\mu}{\sqrt{\sigma_1^2+\sigma_2^2}}, \frac{\lambda\Delta_{ik}-\Delta\mu}{\sqrt{\sigma_1^2+\sigma_2^2}}, \frac{\sigma_2^2}{\sigma_1^2+\sigma_2^2}\right)\\ &\quad \underbrace{\to \Psi(0,0,1)}_{\text{as } \varsigma_2\to\infty} = \Phi(0) = \frac{1}{2}\end{aligned} \tag{117}$$

$$\begin{aligned}M_6 &= \iiint_{-\infty}^{\infty} H(x_i-x_j)H(x_i-x_k)\phi_i\psi_j\psi_k\,dx_i dx_j dx_k\\ &= \Psi\left(\frac{\lambda\Delta_{ij}+\Delta\mu}{\sqrt{\sigma_1^2+\sigma_2^2}}, \frac{\lambda\Delta_{ik}+\Delta\mu}{\sqrt{\sigma_1^2+\sigma_2^2}}, \frac{\sigma_1^2}{\sigma_1^2+\sigma_2^2}\right)\\ &\quad \underbrace{\to \Psi(0,0,0)}_{\text{as } \varsigma_2\to\infty} = \Phi^2(0) = \frac{1}{4}\end{aligned} \tag{118}$$

$$\begin{aligned}M_7 &= \iiint_{-\infty}^{\infty} H(x_i-x_j)H(x_i-x_k)\psi_i\phi_j\psi_k\,dx_i dx_j dx_k\\ &= \Psi\left(\frac{\lambda\Delta_{ij}-\Delta\mu}{\sqrt{\sigma_1^2+\sigma_2^2}}, \frac{\lambda\Delta_{ik}}{\sqrt{2}\sigma_2}, \frac{\sigma_2}{\sqrt{2}\sqrt{\sigma_1^2+\sigma_2^2}}\right)\\ &\quad \underbrace{\to \Psi\left(0, 0, \frac{1}{\sqrt{2}}\right)}_{\text{as } \varsigma_2\to\infty} = \frac{3}{8}\end{aligned} \tag{119}$$

$$M_8 = \int_{-\infty}^{\infty}\!\!\int\!\!\int H(x_i-x_j)H(x_i-x_k)\psi_i\psi_j\phi_k dx_i dx_j dx_k$$
$$= \Psi\left(\frac{\lambda\Delta_{ij}}{\sqrt{2}\sigma_2}, \frac{\lambda\Delta_{ik}-\Delta\mu}{\sqrt{\sigma_1^2+\sigma_2^2}}, \frac{\sigma_2}{\sqrt{2}\sqrt{\sigma_1^2+\sigma_2^2}}\right)$$
$$\to \underbrace{\Psi\left(0, 0, \frac{1}{\sqrt{2}}\right)}_{\text{as } \varsigma_2\to\infty} = \frac{3}{8}. \tag{120}$$

Note that in the above derivations, we have employed the Sheppard's Theorem [46]

$$\Psi(0, 0, \rho) = \frac{1}{4} + \frac{1}{2\pi}\arcsin\rho.$$

Now all quantities needed to calculate $\mathbb{C}(H_{ij}, H_{ik})$ in (110) are ready. Substituting (113)–(120) into (112) and subtracting the product of $\mathbb{E}(H_{ij})$ in (106) and $\mathbb{E}(H_{ik})$ in (107) from the result, it follows that

$$\mathbb{C}(H_{ij}, H_{ik}) = (1-\varepsilon)^3\left(\Psi_{ijk} - \Phi_{ij}\Phi_{ik}\right) + \varepsilon(1-\varepsilon)^3\left(\Phi_{ij}-\frac{1}{2}\right)\left(\Phi_{ik}-\frac{1}{2}\right) + \frac{1}{12}[1-(1-\varepsilon)^3]. \tag{121}$$

Substituting (109) and (121) into (15) and tidying up, we finally arrive at (33), thus completing the proof. □

APPENDIX G
PROOF OF COROLLARY 1

Proof: From (30),

$$\Phi_{ij}(-\lambda) = \Phi\left(\frac{-\lambda\Delta_{ij}}{\sqrt{2}\sigma_1}\right) = 1-\Phi_{ij}. \tag{122}$$

Substituting this relationship into (32) yields

$$\mathbb{E}(T_{\text{GC}}; -\lambda) = (1-\varepsilon)^2\sum_{i\neq j=1}^{n}\sum^{n}(1-\Phi_{ij})\Delta_{ij} \tag{123}$$
$$= \underbrace{-(1-\varepsilon)^2\sum_{i\neq j=1}^{n}\sum^{n}\Phi_{ij}\Delta_{ij}}_{=-\mathbb{E}(T_{\text{GC}})} + \underbrace{(1-\varepsilon)^2\sum_{i\neq j=1}^{n}\sum^{n}\Delta_{ij}}_{=0} \tag{124}$$

which verifies the odd symmetry of $\mathbb{E}(T_{\text{GC}})$.

From (31),

$$\Psi_{ijk}(-\lambda) = \Psi\left(\frac{-\lambda\Delta_{ij}}{\sqrt{2}\sigma_1}, \frac{-\lambda\Delta_{ik}}{\sqrt{2}\sigma_1}, \frac{1}{2}\right)$$

which, by result in [45], is

$$\Psi_{ijk}(-\lambda) = \Psi_{ijk} - \Phi_{ij} - \Phi_{ik} + 1. \tag{125}$$

Replacing λ with $-\lambda$ in (33) and using (122) and (125), it is not difficult to verify that $\mathbb{V}(T_{\text{GC}}; -\lambda) = \mathbb{V}(T_{\text{GC}}; \lambda)$, and the even symmetry thus follows. □

APPENDIX H
PROOF OF THEOREM 2

Proof: Noticing the relationship of $\text{sign}(\cdot) = 2H(\cdot) - 1$, it follows, by taking the expectation on both sides of (8), that

$$\mathbb{E}(T_{\text{SC}}) = \sum_{i=1}^{n}\{2\mathbb{E}[H(X_i)] - 1\}\, y_i \tag{126}$$

where

$$\mathbb{E}[H(X_i)] = (1-\varepsilon)\int_0^{\infty}\phi_i(x)dx + \varepsilon\int_0^{\infty}\psi_i(x)dx$$
$$= (1-\varepsilon)\left[1-\Phi\left(\frac{-\lambda y_i-\mu_1}{\sigma_1}\right)\right] + \varepsilon\Bigg[1-\underbrace{\Phi\left(\frac{-\lambda y_i-\mu_2}{\sigma_2}\right)}_{\to\frac{1}{2}\text{ as }\sigma_2\to\infty}\Bigg]$$
$$= (1-\varepsilon)\Phi\left(\frac{\lambda y_i+\mu_1}{\sigma_1}\right) + \frac{\varepsilon}{2}. \tag{127}$$

Substituting (127) into (126) leads directly to (54).

As to $\mathbb{V}(SC)$, it follows that

$$\mathbb{V}(T_{\text{SC}}) = \mathbb{C}\left\{\sum_i[2H(X_i)-1]y_i, \sum_j[2H(X_j)-1]y_j\right\}$$
$$= 4\sum_i\sum_j\mathbb{C}[H(X_i), H(X_j)]y_iy_j$$
$$= 4\sum_{i\neq j=1}^{n}\sum^{n}\underbrace{\mathbb{C}[H(X_i), H(X_j)]}_{=0\text{ due to i.i.d. assumption}}y_iy_j + 4\sum_i\mathbb{V}[H(X_i)]y_i^2$$
$$= 4\sum_i\left\{\mathbb{E}[H(X_i)] - \mathbb{E}^2[H(X_i)]\right\}y_i^2 \tag{128}$$

where the last step (128) results in (55) upon substitution of (127). This completes the proof. □

REFERENCES

[1] X. Zhu, T. Wang, Y. Bao, F. Hu, and S. Li, "Signal detection in generalized Gaussian distribution noise with Nakagami fading channel," *IEEE Access*, vol. 7, pp. 23120–23126, 2019.
[2] Z. Shang, X. Li, Y. Liu, Y. Wang, and W. Liu, "GLRT detector based on knowledge aided covariance estimation in compound Gaussian environment," *Signal Process.*, vol. 155, pp. 377–383, Feb. 2019.
[3] S. Bartoletti, W. Dai, A. Conti, and M. Z. Win, "A mathematical model for wideband ranging," *IEEE J. Sel. Topics Signal Process.*, vol. 9, no. 2, pp. 216–228, Mar. 2015.
[4] V. G. Chavali and C. R. C. M. da Silva, "Detection of digital amplitude-phase modulated signals in symmetric alpha-stable noise," *IEEE Trans. Commun.*, vol. 60, no. 11, pp. 3365–3375, Nov. 2012.
[5] K. R. Kolodziejski and J. W. Betz, "Detection of weak random signals in IID non-Gaussian noise," *IEEE Trans. Commun.*, vol. 48, no. 2, pp. 222–230, Feb. 2000.
[6] B. M. Sadler, "Detection in correlated impulsive noise using fourth-order cumulants," *IEEE Trans. Signal Process.*, vol. 44, no. 11, pp. 2793–2800, Nov. 1996.
[7] S. M. Kay, *Fundamentals of Statistical Processing* (Prentice-Hall Signal Processing Series). Upper Saddle River, NJ, USA: Prentice-Hall, 1998.

[8] A. W. van der Vaart, *Asymptotic Statistics*. Cambridge, U.K.: Cambridge Univ. Press, 1998.
[9] D. Middleton, "Man-made noise in urban environments and transportation systems: Models and measurements," *IEEE Trans. Commun.*, vol. 21, no. 11, pp. 1232–1241, Nov. 1973.
[10] A. M. Zoubir, V. Koivunen, Y. Chakhchoukh, and M. Muma, "Robust estimation in signal processing: A tutorial-style treatment of fundamental concepts," *IEEE Signal Process. Mag.*, vol. 29, no. 4, pp. 61–80, Jul. 2012.
[11] S. A. Kassam and H. V. Poor, "Robust techniques for signal processing: A survey," *Proc. IEEE*, vol. 73, no. 3, pp. 433–481, Mar. 1985.
[12] G. Zhang, J. Wang, G. Yang, Q. Shao, and S. Li, "Nonlinear processing for correlation detection in symmetric alpha-stable noise," *IEEE Signal Process. Lett.*, vol. 25, no. 1, pp. 120–124, Jan. 2018.
[13] H. Oh and H. Nam, "Design and performance analysis of nonlinearity preprocessors in an impulsive noise environment," *IEEE Trans. Veh. Technol.*, vol. 66, no. 1, pp. 364–376, Jan. 2017.
[14] A. Mahmood, M. Chitre, and H. Vishnu, "Locally optimal inspired detection in snapping shrimp noise," *IEEE J. Ocean. Eng.*, vol. 42, no. 4, pp. 1049–1062, Oct. 2017.
[15] H. Oh, H. Nam, and S. Park, "Adaptive threshold blanker in an impulsive noise environment," *IEEE Trans. Electromagn. Compat.*, vol. 56, no. 5, pp. 1045–1052, Oct. 2014.
[16] F. H. Juwono, Q. Guo, D. Huang, and K. P. Wong, "Deep clipping for impulsive noise mitigation in OFDM-based power-line communications," *IEEE Trans. Power Del.*, vol. 29, no. 3, pp. 1335–1343, Jun. 2014.
[17] P. P. Pokharel, W. Liu, and J. C. Principe, "A low complexity robust detector in impulsive noise," *Signal Process.*, vol. 89, no. 10, pp. 1902–1909, 2009.
[18] G. Guo, M. Mandal, and Y. Jing, "A robust detector of known signal in non-Gaussian noise using threshold systems," *Signal Process.*, vol. 92, no. 11, pp. 2676–2688, 2012.
[19] Z. Luo and Y. Zhang, "Novel nonlinearity based on gaussianization and generalized matching for impulsive noise suppression," *IEEE Access*, vol. 7, pp. 65163–65173, 2019.
[20] G. A. Tsihrintzis and C. L. Nikias, "Performance of optimum and suboptimum receivers in the presence of impulsive noise modeled as an alpha-stable process," *IEEE Trans. Commun.*, vol. 43, no. 234, pp. 904–914, Feb. 1995.
[21] T. S. Saleh, I. Marsland, and M. El-Tanany, "Suboptimal detectors for alpha-stable noise: Simplifying design and improving performance," *IEEE Trans. Commun.*, vol. 60, no. 10, pp. 2982–2989, Oct. 2012.
[22] W. Xu, C. Chen, J. Dai, Y. Zhou, and Y. Zhang, "Detection of known signals in additive impulsive noise based on spearman's rho and Kendall's tau," *Signal Process.*, vol. 161, pp. 165–179, Aug. 2019.
[23] N. Beaulieu and C. Leung, "Optimal detection of hard-limited data signals in different noise environments," *IEEE Trans. Commun.*, vol. 34, no. 6, pp. 619–622, Jun. 1986.
[24] S. Kassam and J. Thomas, "Asymptotically robust detection of a known signal in contaminated non-Gaussian noise," *IEEE Trans. Inf. Theory*, vol. 22, no. 1, pp. 22–26, Jan. 1976.
[25] E. Schezhtman and S. Yitzhaki, "A measure of association based on gin's mean difference," *Commun. Statist.-Theory Methods*, vol. 16, no. 1, pp. 207–231, 1987.
[26] W. Xu, Y. Hung, M. Niranjan, and M. Shen, "Asymptotic mean and variance of Gini correlation for bivariate normal samples," *IEEE Trans. Signal Process.*, vol. 58, no. 2, pp. 522–534, Feb. 2010.
[27] W. Xu, R. Ma, Y. Zhou, S. Peng, and Y. Hou, "Asymptotic properties of Pearson's rank-variate correlation coefficient in bivariate normal model," *Signal Process.*, vol. 119, pp. 190–202, Feb. 2016.
[28] R. Ma, W. Xu, Y. Zhang, and Z. Ye, "Asymptotic properties of Pearson's rank-variate correlation coefficient under contaminated Gaussian model," *PLoS One*, vol. 9, no. 11, 2014, Art. no. e112215.
[29] G. E. Noether, "On a theorem of pitman," *Ann. Math. Statist.*, vol. 26, no. 1, pp. 64–68, 1955.
[30] S. M. Kay, *Fundamentals of Statistical Signal Processing: Detection Theory*. Upper Saddle River, NJ, USA: Prentice-Hall, 1998.
[31] C. Nikias and M. Shoa, "Signal processing with alpha-stable distributions and applications," *Comput. Statist. Data Anal.*, vol. 22, no. 3, p. 334, 1996.
[32] D. Middleton, "Statistical-physical models of electromagnetic interference," *IEEE Trans. Electromagn. Compat.*, vol. 19, no. 3, pp. 106–127, Aug. 1977.
[33] D. Middleton, "Non-Gaussian noise models in signal processing for telecommunications: New methods an results for class A and class B noise models," *IEEE Trans. Inf. Theory*, vol. 45, no. 4, pp. 1129–1149, May 1999.
[34] X. T. Li, J. Sun, L. W. Jin, and M. Liu, "Bi-parameter CGM model for approximation of α-stable PDF," *Electron. Lett.*, vol. 44, no. 18, pp. 1096–1097, Aug. 2008.
[35] A. Kadri, "Suboptimal receivers for weak M-ary chirp signals in non-Gaussian noise," in *Proc. 20th European Wireless Conf.*, May 2014, pp. 1–6.
[36] S. V. Zhidkov, "Performance analysis and optimization of OFDM receiver with blanking nonlinearity in impulsive noise environment," *IEEE Trans. Veh. Technol.*, vol. 55, no. 1, pp. 234–242, Jan. 2006.
[37] E. Alsusa and K. M. Rabie, "Dynamic peak-based threshold estimation method for mitigating impulsive noise in power-line communication systems," *IEEE Trans. Power Del.*, vol. 28, no. 4, pp. 2201–2208, Oct. 2013.
[38] S.-C. Chan and Y.-X. Zou, "A recursive least M-estimate algorithm for robust adaptive filtering in impulsive noise: Fast algorithm and convergence performance analysis," *IEEE Trans. Signal Process.*, vol. 52, no. 4, pp. 975–991, Apr. 2004.
[39] W. Xu, C. Chang, Y. S. Hung, S. K. Kwan, and P. C. W. Fung, "Order statistics correlation coefficient as a novel association measurement with applications to biosignal analysis," *IEEE Trans. Signal Process.*, vol. 55, no. 12, pp. 5552–5563, Dec. 2007.
[40] W. Xu, J. Dai, Y. Hung, and Q. Wang, "Estimating the area under a receiver operating characteristic (ROC) curve: Parametric and nonparametric ways," *Signal Process.*, vol. 93, no. 11, pp. 3111–3123, Nov. 2013.
[41] R. Ma, W. Xu, Q. Wang, and W. Chen, "Robustness analysis of three classical correlation coefficients under contaminated Gaussian model," *Signal Process.*, vol. 104, pp. 51–58, Nov. 2014.
[42] R. Ma, W. Xu, S. Liu, Y. Zhang, and J. Xiong, "Asymptotic mean and variance of Gini correlation under contaminated Gaussian model," *IEEE Access*, vol. 4, pp. 8095–8104, 2016.
[43] W. Xu, Y. Hou, Y. S. Hung, and Y. Zou, "A comparative analysis of Spearman's rho and Kendall's tau in normal and contaminated normal models," *Signal Process.*, vol. 93, no. 1, pp. 261–276, 2013.
[44] M. Kendall and J. D. Gibbons, *Rank Correlation Methods*, 5th ed. New York, NY, USA: Oxford Univ. Press, 1990.
[45] Z. Drezner, "Computation of the bivariate normal integral," *Math. Comput.*, vol. 32, no. 141, pp. 277–279, 1978.
[46] P. A. Moran, "Rank correlation and product-moment correlation," *Biometrika*, vol. 36, nos. 1–2, pp. 203–206, 1948.

CHANGRUN CHEN received the B.Eng. degree in automation from the School of Automation, Guangdong University of Technology, Guangzhou, China, in 2017, where he is currently pursuing the Ph.D. degree. His research interests include signal processing, machine learning, and wireless communications.

WEICHAO XU (M'06) received the B.Eng. and M.Eng. degrees in electrical engineering from the University of Science and Technology of China, Hefei, in 1993 and 1996, respectively, and the Ph.D. degree in biomedical engineering from The University of Hong Kong, Hong Kong, in 2002. He was a Research Associate with the Department of Electrical and Electronic Engineering, The University of Hong Kong, from 2002 to 2010. In 2011, he entered the 100-Talent Scheme with the Guangdong University of Technology, where he is currently a Professor. His research interests are in the areas of mathematical statistics, computational statistics, information theory, machine learning, optimization theory, digital signal processing, and applications.

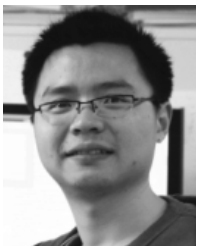

JISHENG DAI (S'08–M'11) received the B.Eng. degree in electrical engineering from the Nanjing University of Technology, Nanjing, China, in 2005, and the Ph.D. degree in information and communication engineering from the University of Science and Technology of China, Hefei, China, in 2010. He was a Research Assistant with the Department of Electrical and Electronic Engineering, The University of Hong Kong, Hong Kong, in 2009. He is currently a Research Associate with the School of Electrical and Information Engineering, Jiangsu University, Zhenjiang, China. His research interests are in the areas of convex optimization theory, information theory, wireless communications, machine learning, and bioinformatics.

YANZHOU ZHOU received the B.S. and M.S. degrees from the Harbin Institute of Technology, Harbin, China, in 1981 and 1992, respectively, and the Ph.D. degree in optical engineering from Loughborough University, U.K., in 2007. He is currently a Professor with the School of Automation, Guangdong University of Technology, Guangzhou, Guangdong, China. His research interests include optical signal and image processing, and mechanical measurement.

YUN ZHANG received the B.S. and M.S. degrees in automatic engineering from Hunan University, Changsha, China, in 1982 and 1986, respectively, and the Ph.D. degree in automatic engineering from the South China University of Science and Technology, Guangzhou, China, in 1998. He is currently a Professor with the School of Automation, Guangdong University of Technology, Guangzhou, Guangdong, China. His research interests include intelligent control systems, network systems, and signal processing.